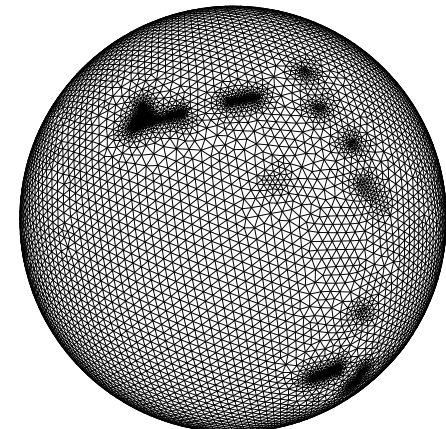
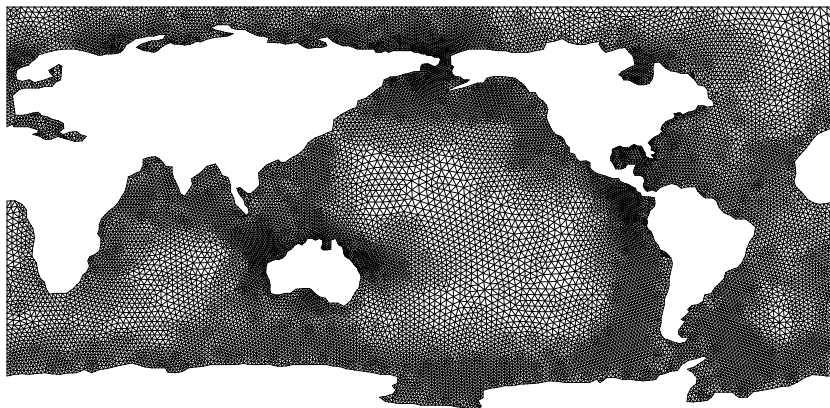


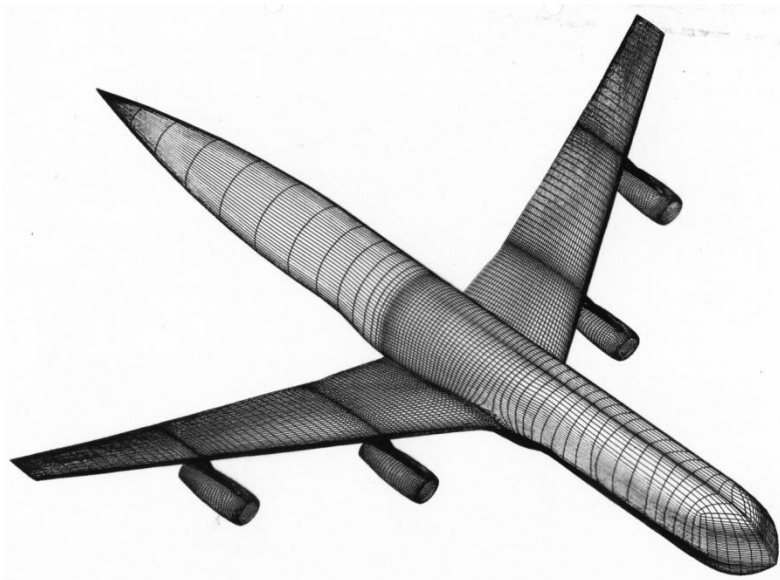
Introduction to element based computing --- finite volume and finite element methods. Mesh generation

*Joanna Szmelter
Loughborough University, UK*

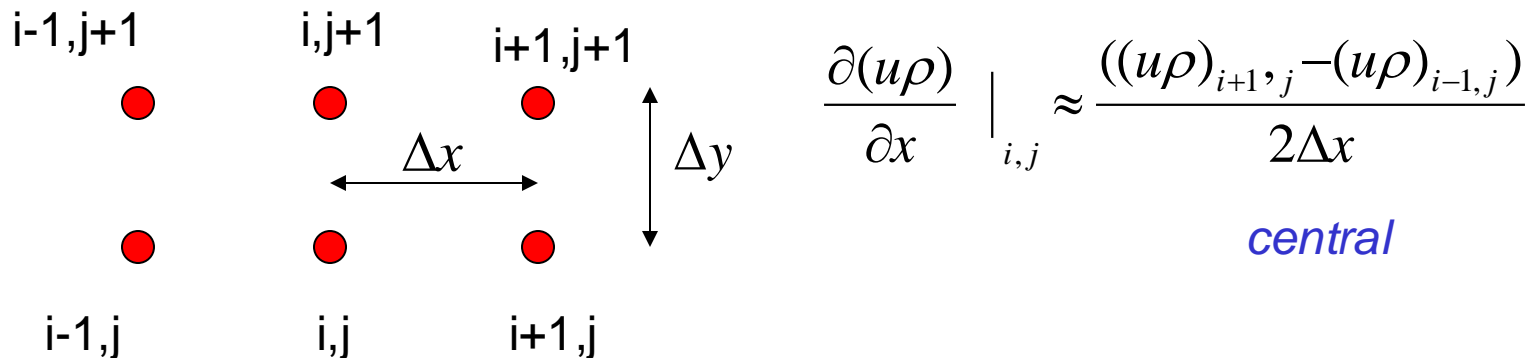


Traditional Discretisation Methods

- Finite Difference
- Finite Element
- Finite Volume



Finite Difference Method



$$\frac{\partial(u\rho)}{\partial x} \Big|_{i,j} \approx \frac{((u\rho)_{i+1,j} - (u\rho)_{i-1,j})}{2\Delta x}$$

central

$O(\Delta x^2)$

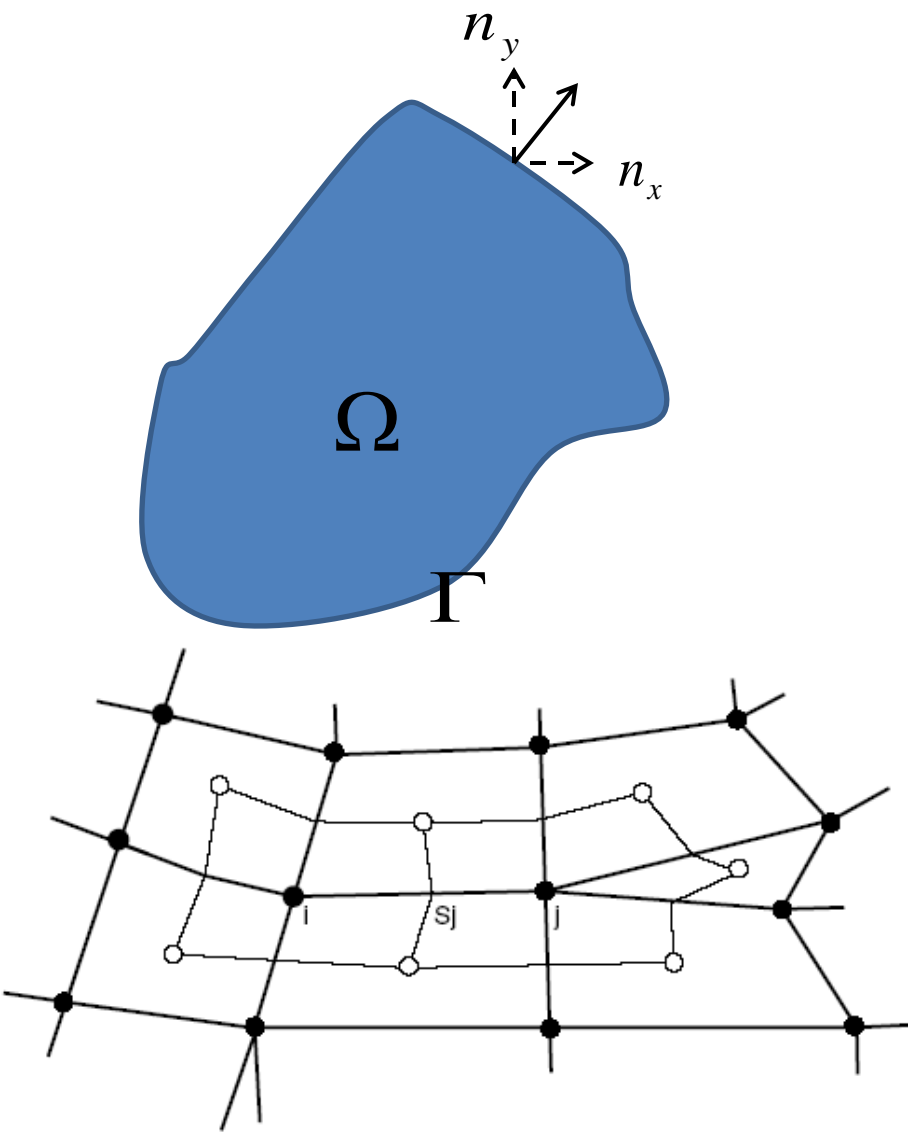
$$\frac{\partial(u\rho)}{\partial x} \Big|_{i,j} \approx \frac{((u\rho)_{i+1,j} - (u\rho)_{i,j})}{\Delta x}$$

forward

$$\frac{\partial \rho}{\partial t} + \frac{\partial(u\rho)}{\partial x} + \frac{\partial(v\rho)}{\partial y} = 0$$

$$\frac{\partial}{\partial t} \rho_{i,j} + \frac{((u\rho)_{i+1,j} - (u\rho)_{i-1,j})}{2\Delta x} + \frac{((v\rho)_{i,j+1} - (v\rho)_{i,j-1})}{2\Delta y} = 0$$

Finite Volume Method

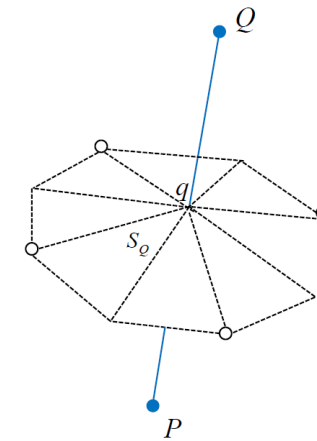


$$\frac{\partial \rho}{\partial t} + \frac{\partial(u\rho)}{\partial x} + \frac{\partial(v\rho)}{\partial y} = 0$$

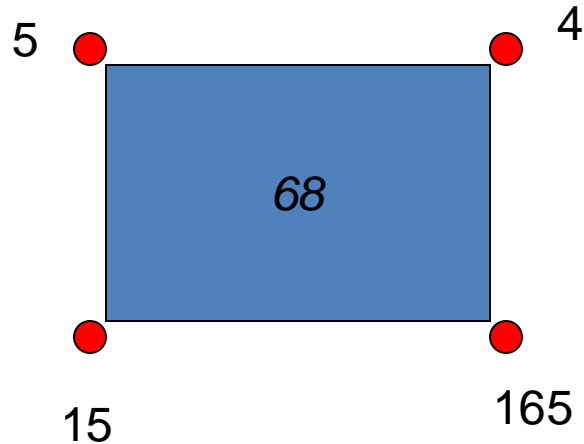
$$\int_{\Omega} \frac{\partial \rho}{\partial t} d\Omega + \int_{\Omega} \frac{\partial(u\rho)}{\partial x} d\Omega + \int_{\Omega} \frac{\partial(v\rho)}{\partial y} d\Omega = 0$$

From Gauss Divergence Theorem:

$$\begin{aligned} \frac{\partial}{\partial t} \int_{\Omega} \rho d\Omega + \int_{\Gamma} (u\rho)n_x d\Gamma + \int_{\Gamma} (v\rho)n_y d\Gamma &= 0 \\ \frac{\partial}{\partial t} \rho_i V_i + \sum_j (u\rho)_{ij} S_x + \sum_i (v\rho)_{ij} S_y &= 0 \end{aligned}$$



Finite Element Method



Element

68

Nodes

5 4 165 15

*(Repeated index
notation is used here)*

$$\rho \approx \rho_i N_i =$$

$$\rho_5 N_5 + \rho_4 N_4 + \rho_{165} N_{165} + \rho_{15} N_{15}$$

$$\frac{\partial \rho}{\partial t} + \frac{\partial(u\rho)}{\partial x} + \frac{\partial(v\rho)}{\partial y} = 0$$

$$\int_{\Omega} \frac{\partial \rho}{\partial t} d\Omega + \int_{\Omega} \frac{\partial(u\rho)}{\partial x} d\Omega + \int_{\Omega} \frac{\partial(v\rho)}{\partial y} d\Omega = 0$$

$$\frac{\partial}{\partial t} \int_{\Omega} \rho_i N_i d\Omega + \int_{\Omega} \frac{\partial(u\rho)_i N_i}{\partial x} d\Omega + \int_{\Omega} \frac{\partial(v\rho)_i N_i}{\partial y} d\Omega = 0$$

Finite Element Method continued

Weighted residual analysis:

$$\frac{\partial}{\partial t} \int_{\Omega} \rho_i N_i W_j d\Omega + \int_{\Omega} \frac{\partial(u\rho)_i N_i}{\partial x} W_j d\Omega + \int_{\Omega} \frac{\partial(v\rho)_i N_i}{\partial y} W_j d\Omega = 0$$

$$\frac{\partial}{\partial t} \left(\int_{\Omega} N_i W_j d\Omega \right) \rho_i + \left(\int_{\Omega} \frac{\partial(N_i)}{\partial x} W_j d\Omega \right) u \rho_i + \left(\int_{\Omega} \frac{\partial(N_i)}{\partial y} W_j d\Omega \right) v \rho_i = 0$$

If W is chosen to be the same as N the method is called Galerkin method.

$$\frac{\partial}{\partial t} \left(\int_{\Omega} N_i N_j d\Omega \right) \rho_i + \left(\int_{\Omega} \frac{\partial(N_i)}{\partial x} N_j d\Omega \right) u \rho_i + \left(\int_{\Omega} \frac{\partial(N_i)}{\partial y} N_j d\Omega \right) v \rho_i = 0$$

For easy implementation of boundary conditions this is integrated by parts.

$$\begin{aligned} \frac{\partial}{\partial t} \left(\int_{\Omega} N_i N_j d\Omega \right) \rho_i - \left(\int_{\Omega} N_i \frac{\partial(N_j)}{\partial x} d\Omega \right) u \rho_i - \left(\int_{\Omega} N_i \frac{\partial(N_j)}{\partial y} d\Omega \right) v \rho_i + \left(\int_{\Gamma} N_i N_j n_x d\Gamma \right) u \rho_i + \left(\int_{\Gamma} N_i N_j n_y d\Gamma \right) v \rho_i &= 0 \\ \frac{\partial}{\partial t} \mathbf{M}_{elem} \rho_i + \mathbf{B}_{x elem} u \rho_i + \mathbf{B}_{y elem} v \rho_i &= 0 \end{aligned}$$

Finite Element Method

- 1) Divides computational space into elements

$$\frac{\partial}{\partial t} \mathbf{M}_{elem} \rho_i + \mathbf{B}_{X elem} u \rho_i + \mathbf{B}_{Y elem} v \rho_i = 0$$

For every element constructs

$$\mathbf{M}_{elem}, \mathbf{B}_{X elem}, \mathbf{B}_{Y elem}; \boldsymbol{\rho}_{elem}, \mathbf{u}\boldsymbol{\rho}_{elem}, \mathbf{v}\boldsymbol{\rho}_{elem}$$

- 2) Reconnects elements at nodes

Agglomerates for the whole domain

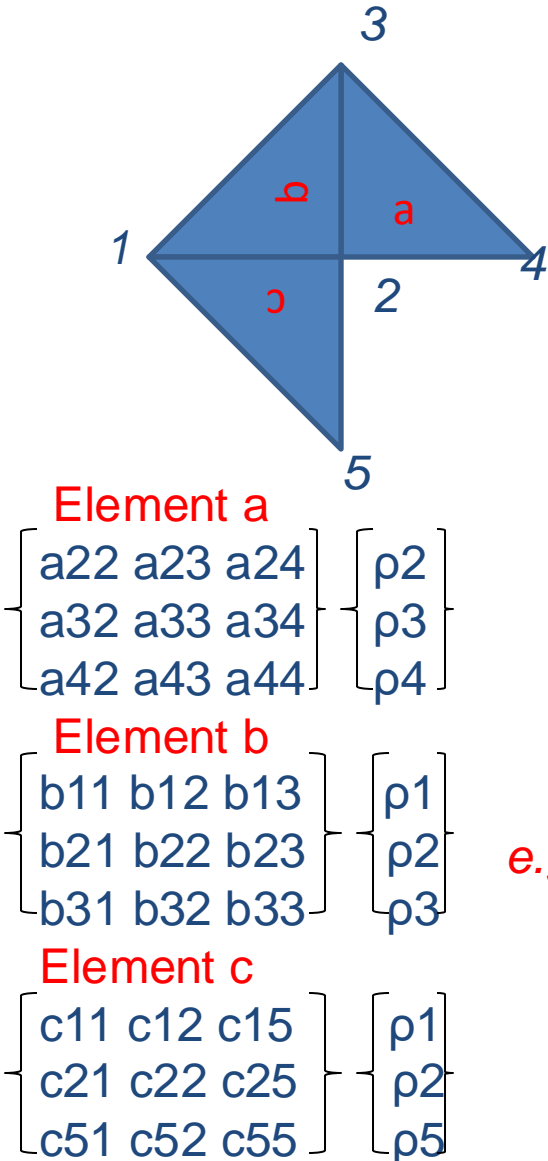
$$\mathbf{M} = \sum_e \mathbf{M}_{elem}, \mathbf{B}_X = \sum_e \mathbf{B}_{X elem}, \mathbf{B}_Y = \sum_e \mathbf{B}_{Y elem}$$

$$\boldsymbol{\rho} = \sum_e \boldsymbol{\rho}_{elem}, \mathbf{u}\boldsymbol{\rho} = \sum_e \mathbf{u}\boldsymbol{\rho}_{elem}, \mathbf{v}\boldsymbol{\rho} = \sum_e \mathbf{v}\boldsymbol{\rho}_{elem}$$

- 3) As a result a set of algebraic equations is formed and its solution follows

$$\frac{\partial}{\partial t} \mathbf{M} \boldsymbol{\rho} + \mathbf{B}_X \mathbf{u}\boldsymbol{\rho} + \mathbf{B}_Y \mathbf{v}\boldsymbol{\rho} = \mathbf{0}$$

Matrix Agglomeration



Global matrix is a sum of all element matrixes

$$\begin{bmatrix} b_{11}+c_{11} & b_{12}+c_{12} & b_{13} & 0 & c_{15} \\ b_{21}+c_{21} & a_{22}+b_{22}+c_{22} & a_{23}+b_{23} & a_{24} & c_{25} \\ b_{31} & a_{32}+b_{32} & a_{33}+b_{33} & a_{34} & 0 \\ 0 & a_{42} & a_{43} & a_{44} & 0 \\ c_{51} & c_{52} & 0 & 0 & c_{55} \end{bmatrix} \begin{bmatrix} p_1 \\ p_2 \\ p_3 \\ p_4 \\ p_5 \end{bmatrix}$$

$$\frac{\partial}{\partial t} \mathbf{M} \boldsymbol{\rho} + \mathbf{B}_x \mathbf{u} \boldsymbol{\rho} + \mathbf{B}_y \mathbf{v} \boldsymbol{\rho} = \mathbf{0}$$

e.g. For the linear triangular element the consistent mass matrix

$$\begin{bmatrix} a_{22} & a_{23} & a_{24} \\ a_{32} & a_{33} & a_{34} \\ a_{42} & a_{43} & a_{44} \end{bmatrix} = \begin{bmatrix} 2 & 1 & 1 \\ 1 & 2 & 1 \\ 1 & 1 & 2 \end{bmatrix} \cdot \frac{\text{Area}}{\text{Element "a" } /12}$$

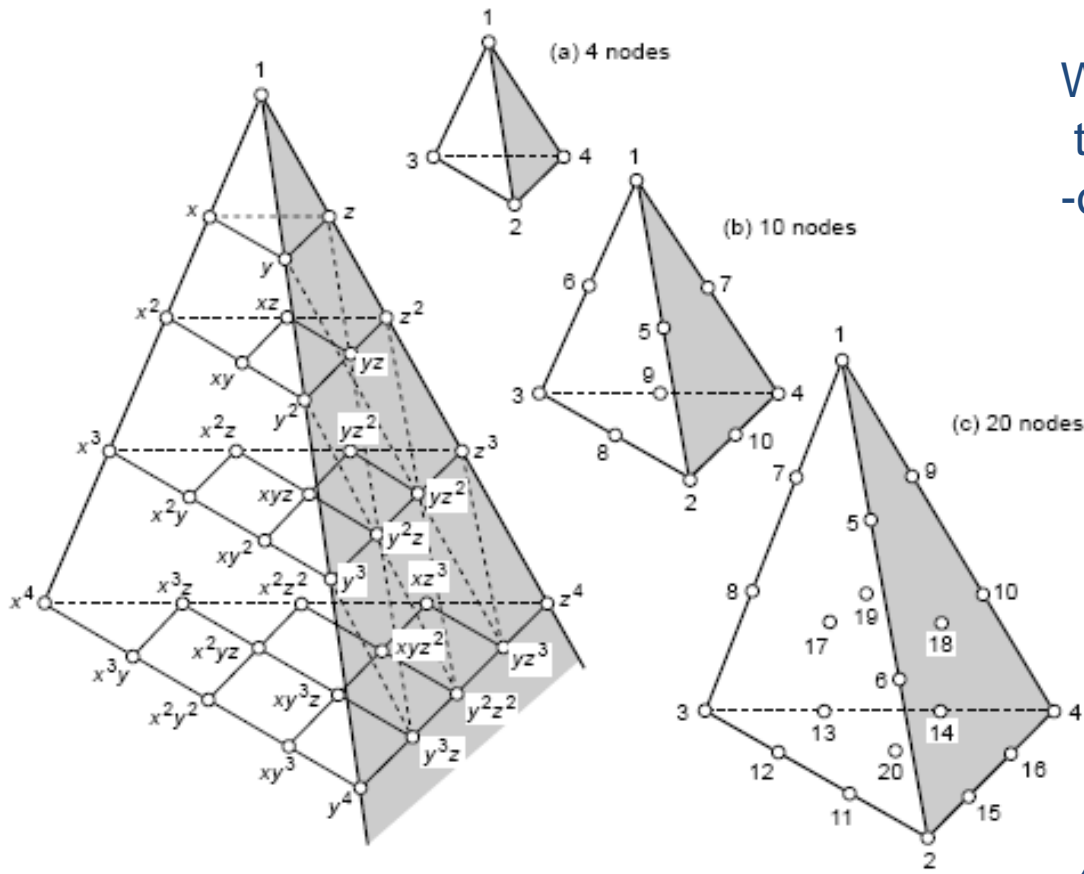
SHAPE FUNCTIONS

$$\rho \approx \sum_i N_i \rho_i$$

And when derivatives are of interest:

$$\frac{d\rho}{dx} \approx \sum_i \frac{dN_i}{dx} \rho_i$$

The tetrahedron family of elements



We know functions N ,
they are frequently polynomials
-obtaining their derivatives is easy.

After Zienkiewicz et al FEM 2000

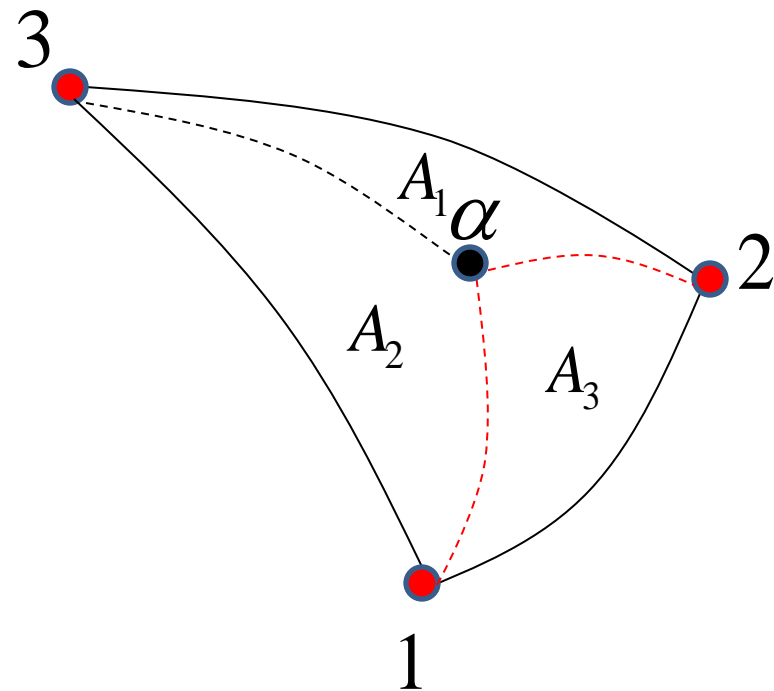
SHAPE FUNCTIONS

Example: a linear interpolation of a scalar T in a triangle. The value of T in an arbitrary point α is approximated by:

$$\rho_\alpha \approx \rho_1 N_1 + \rho_2 N_2 + \rho_3 N_3$$

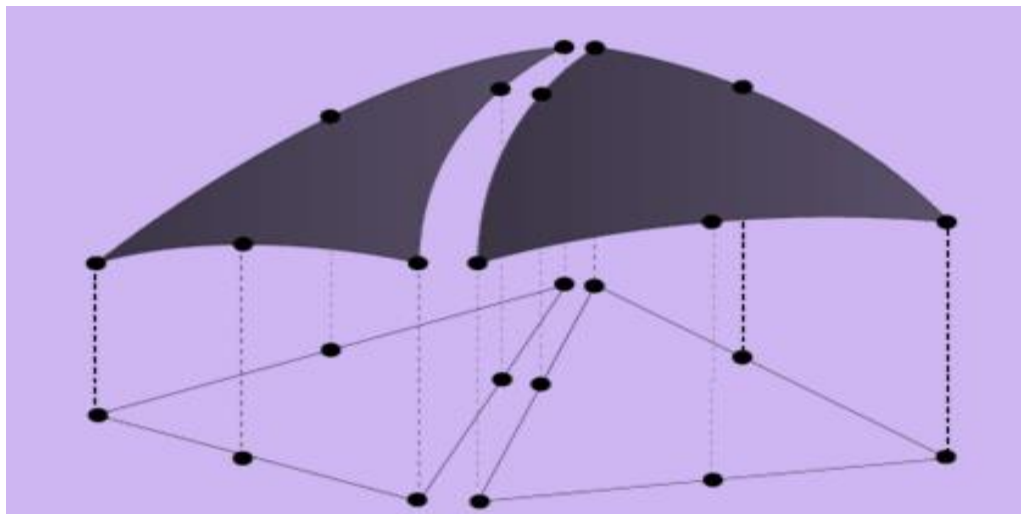
$$N_1 = A_1 / A_{element}$$

where A is an area



SHAPE FUNCTIONS

Curvilinear elements can be formed using transformations



Isoparametric elements

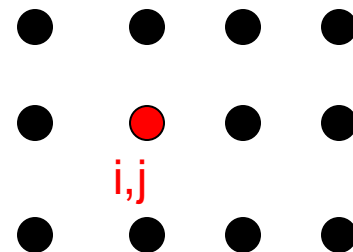
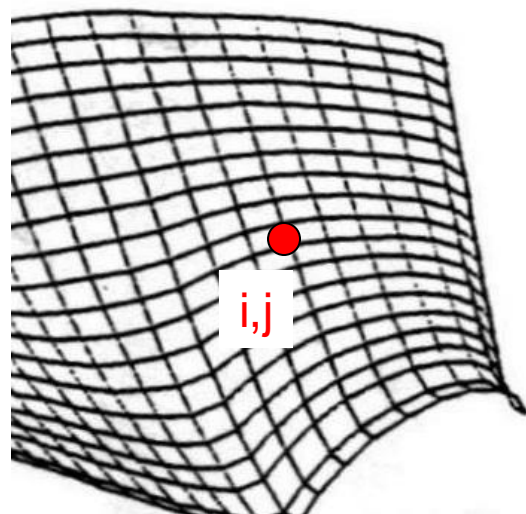
Typical Examples of Data Structures

Structured

Point based --- I,J,K indexing

Set of coordinates and connectivities

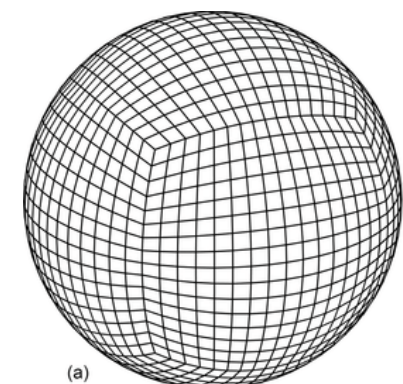
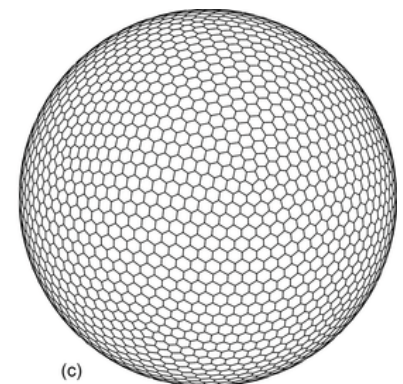
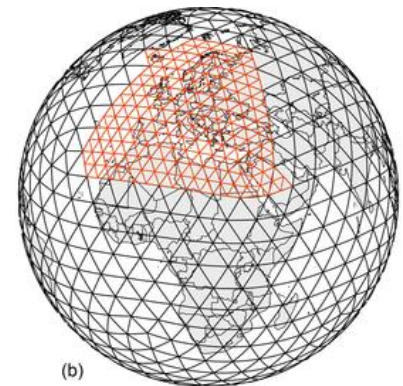
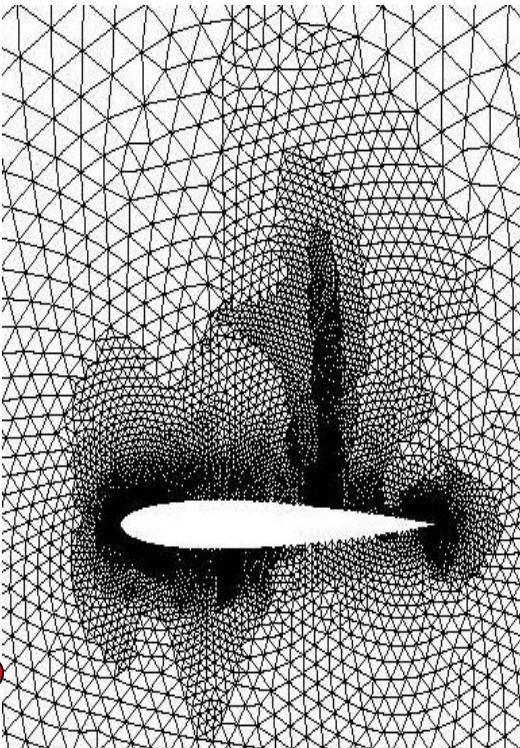
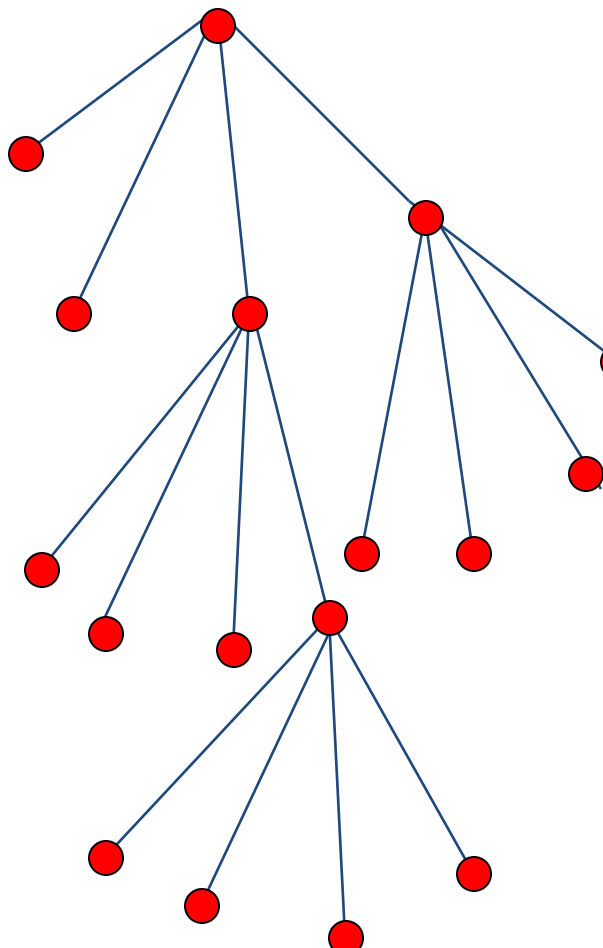
Naturally map into the elements of a matrix



Typical Examples of Data Structures

Structured

Binary trees

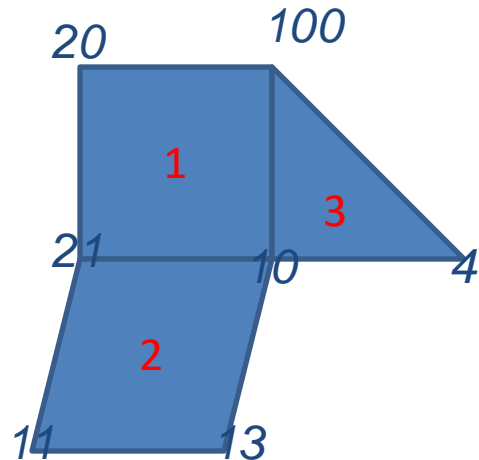


Source: Ullrich et al
GMD 2017

Typical Examples of Data Structures

Unstructured

Element based connectivity

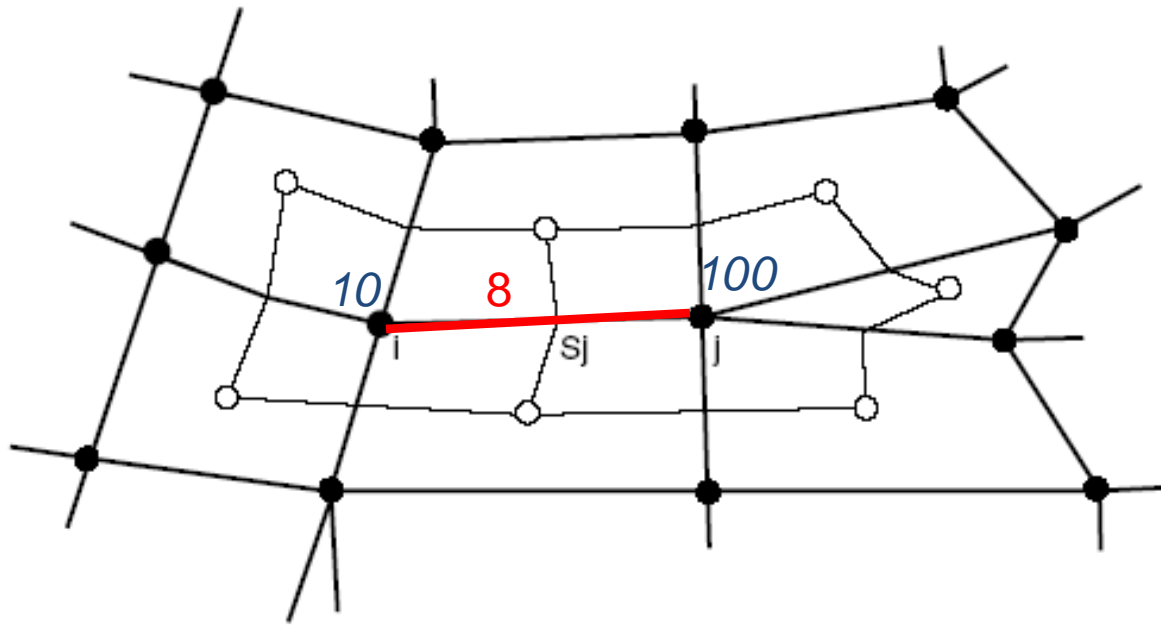


Element 1	10 100 20 21
Element 2	21 11 13 10
Element 3	4 100 10

+ information related to shape functions

Typical Examples of Data Structures

Unstructured

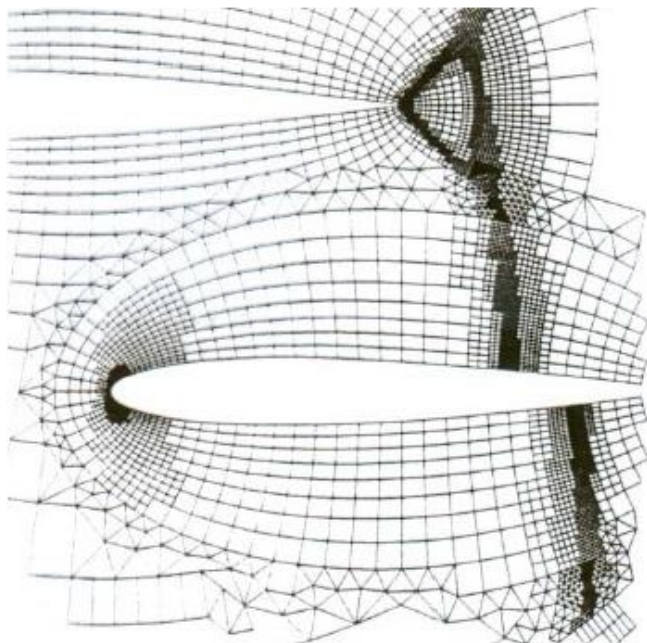


Edge 8 10 100

+ geometrical information

Edge based data

- ☺ *Flexible mesh adaptivity and hybrid meshes*
- ☺ *Low storage*
- ☺ *Easy generalisation to 3D,*
- ☺ *Less expensive than element based data structure*
- ☹  *More expensive operations than I,J,K*



Selected Mesh Generation Techniques

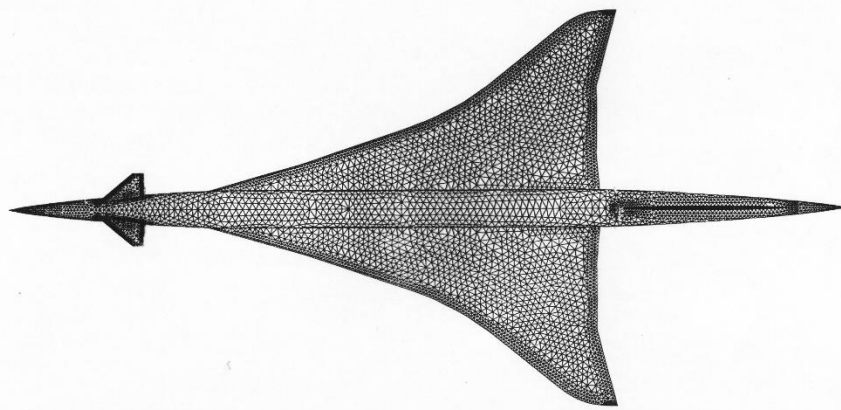
Unstructured Meshes

Direct triangulation

Advancing Front Technique

Delaunay Triangulation

Others

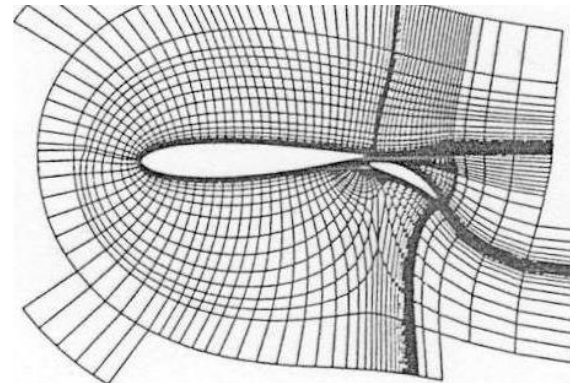


Structured Meshes

Cartesian grids with mapping and/or immersed boundaries

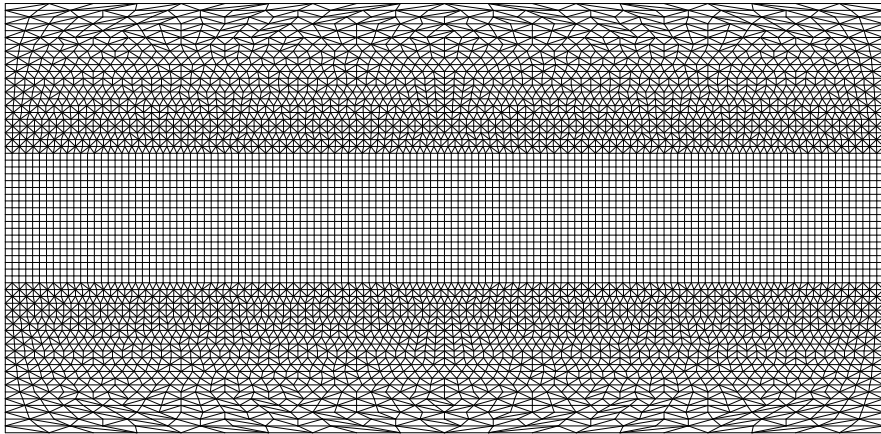
Variants of icosahedral meshes

Others

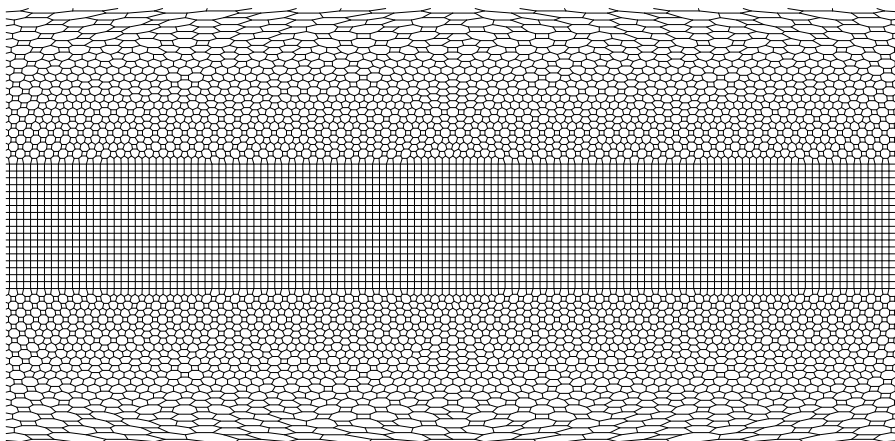


An example of the direct triangulation

Reduced Gaussian Grid

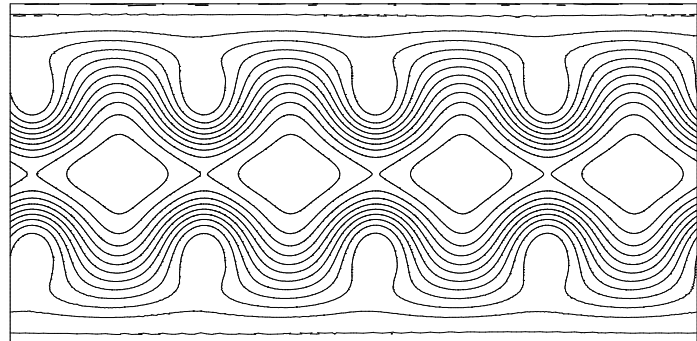


Primary mesh

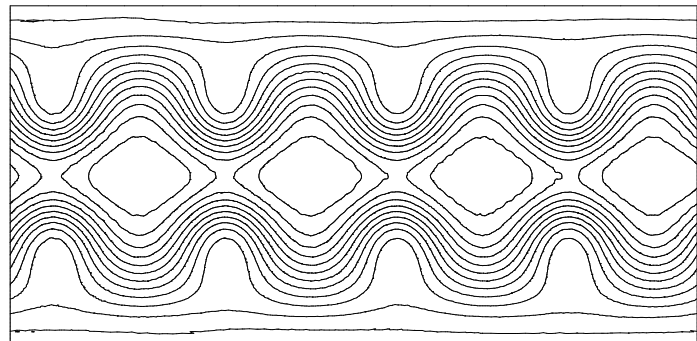


Dual mesh

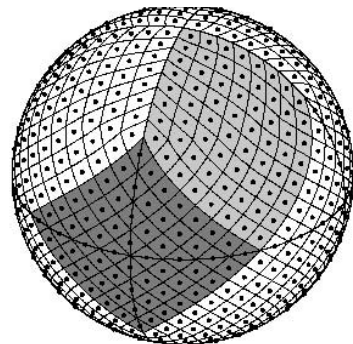
Rossby-Haurwitz Wave



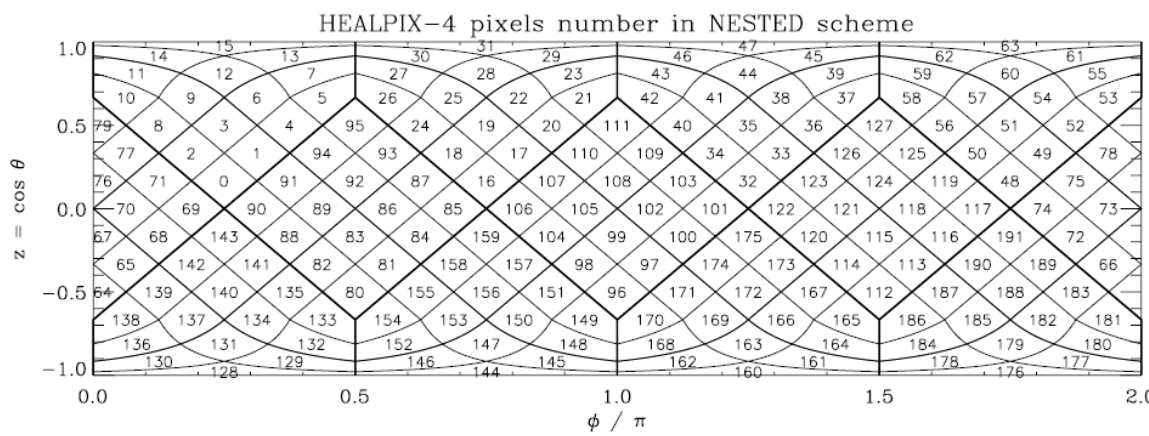
5 days



14 days

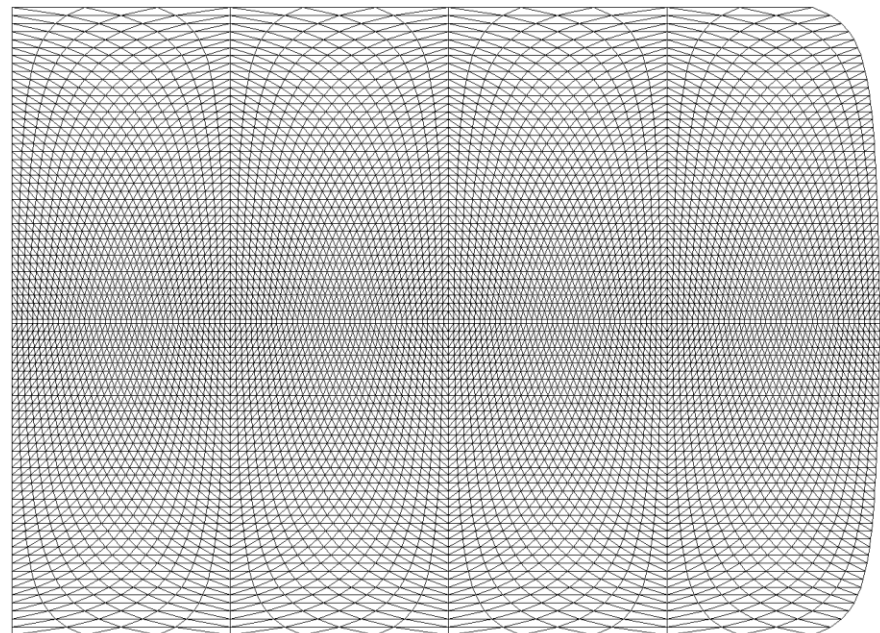
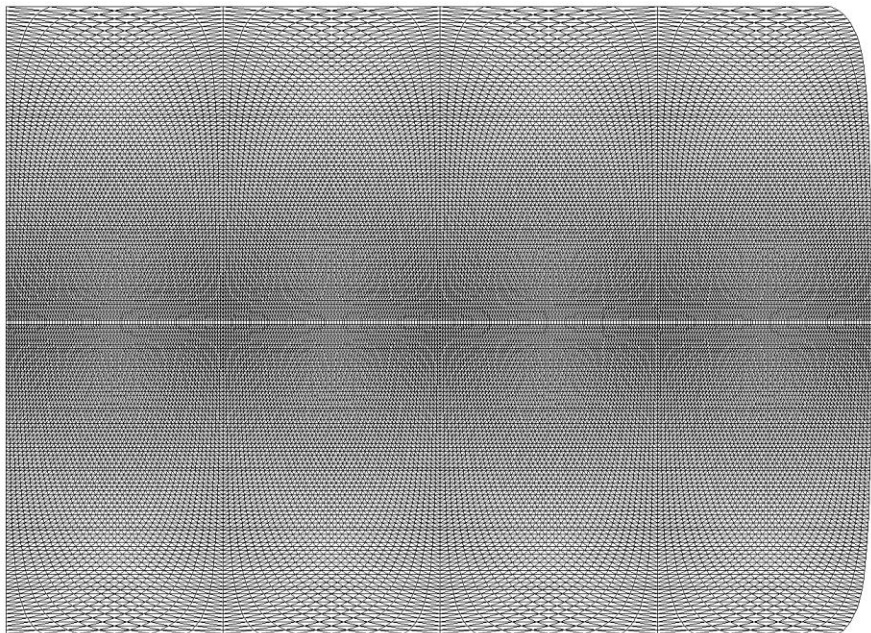


An example of bespoke mesh



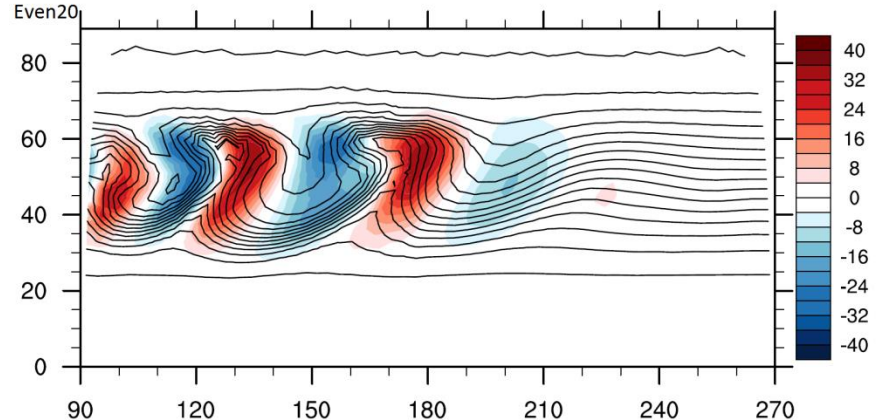
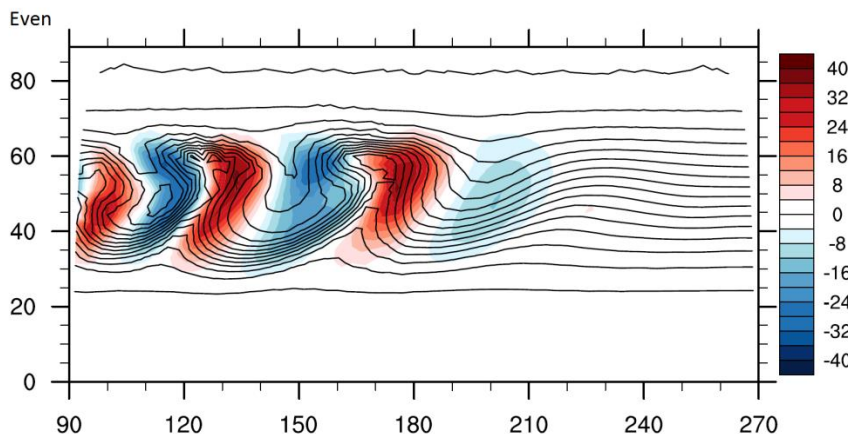
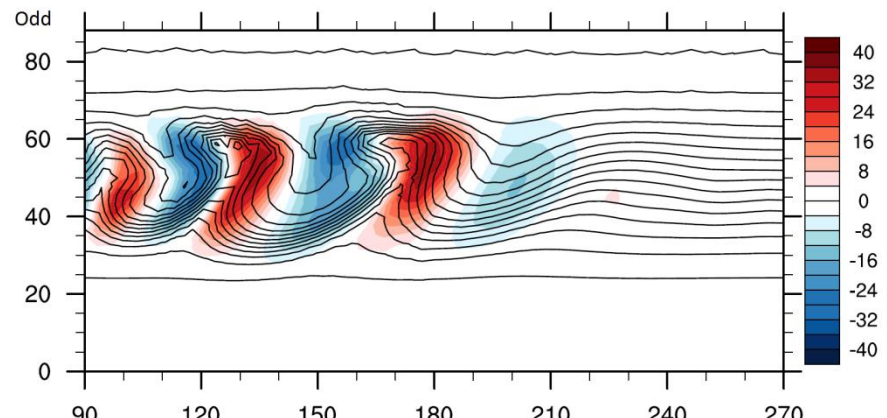
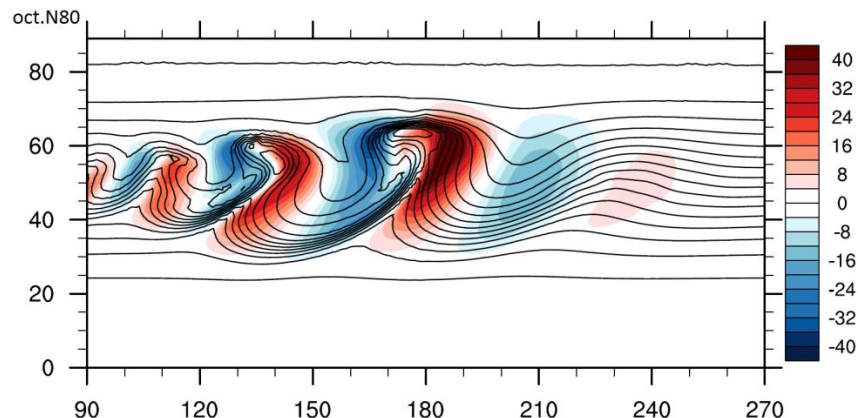
Source: Gorski et al
Astrophysical Journal 2005

Oct.N80 and reduced meshes



Oct.N80 fine and 'odd' reduced meshes

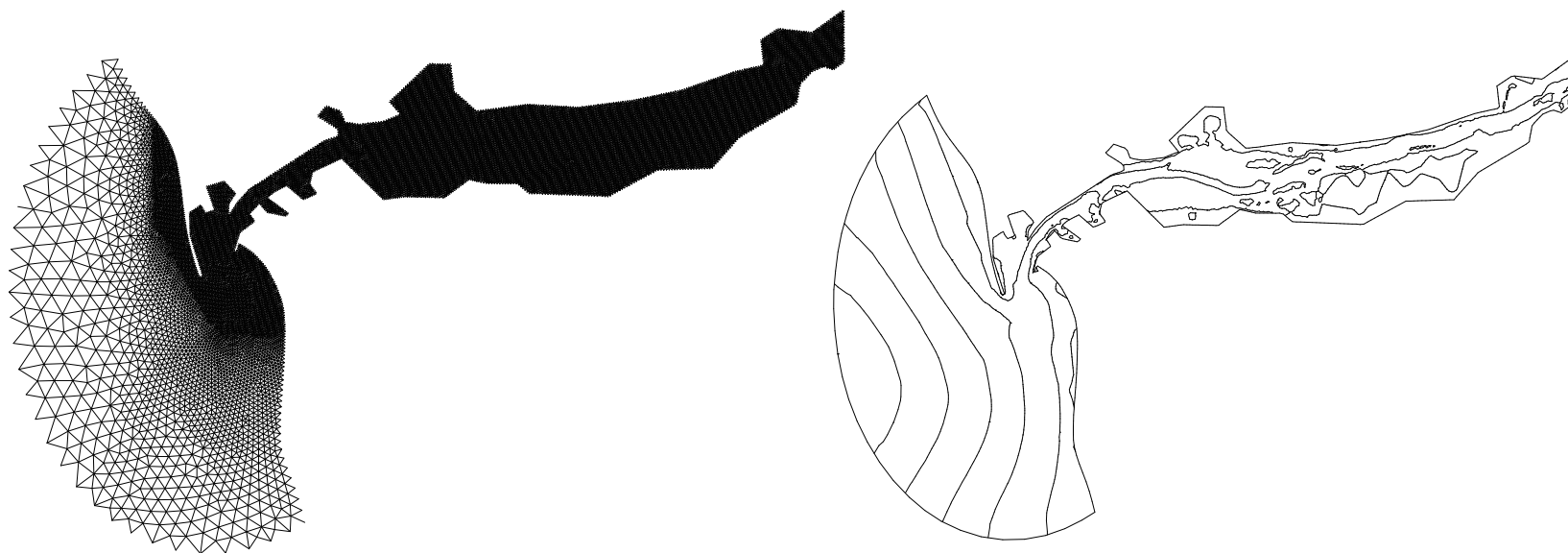
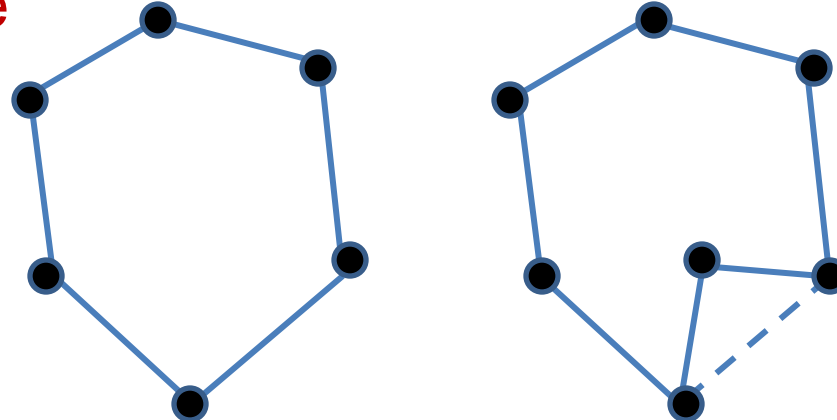
Reduced Mesh – Baroclinic Instability



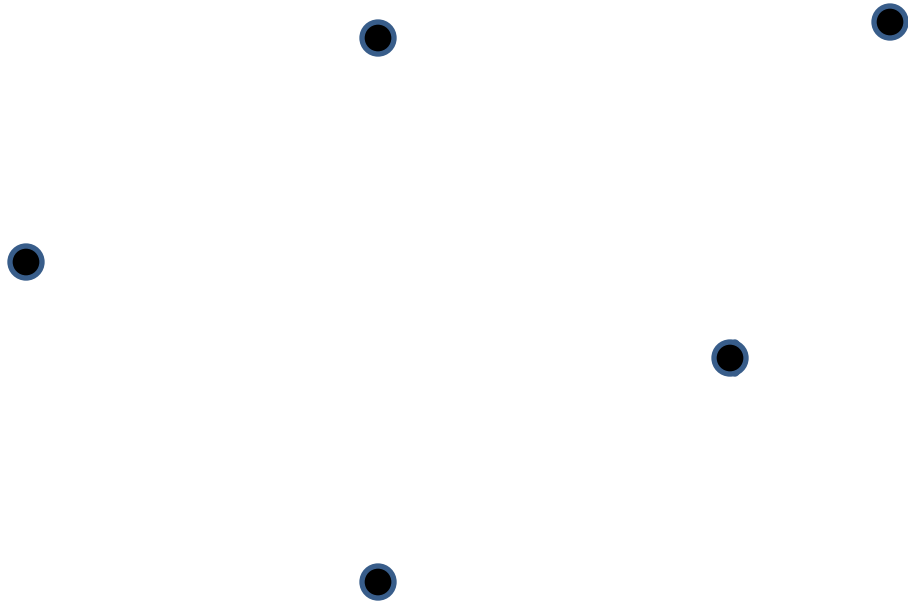
Day 8, horizontal velocity and potential
temperature

Advancing Front Technique

Simultaneous mesh point generation and connectivity

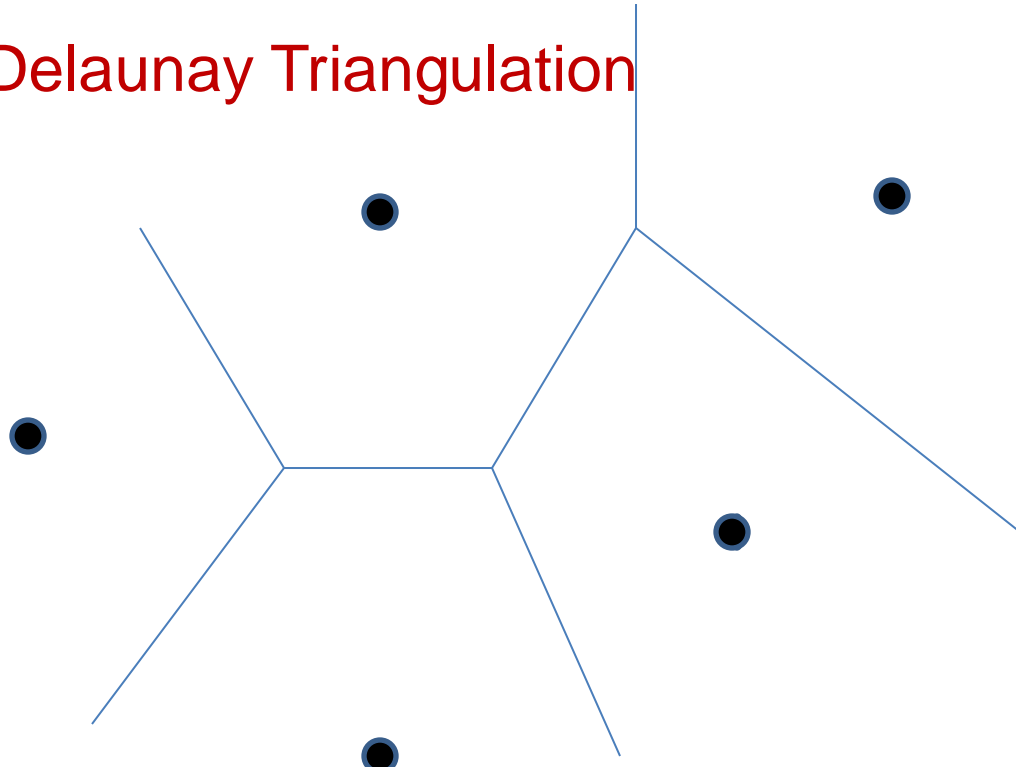


Delaunay Triangulation



How to connect a given set of points?

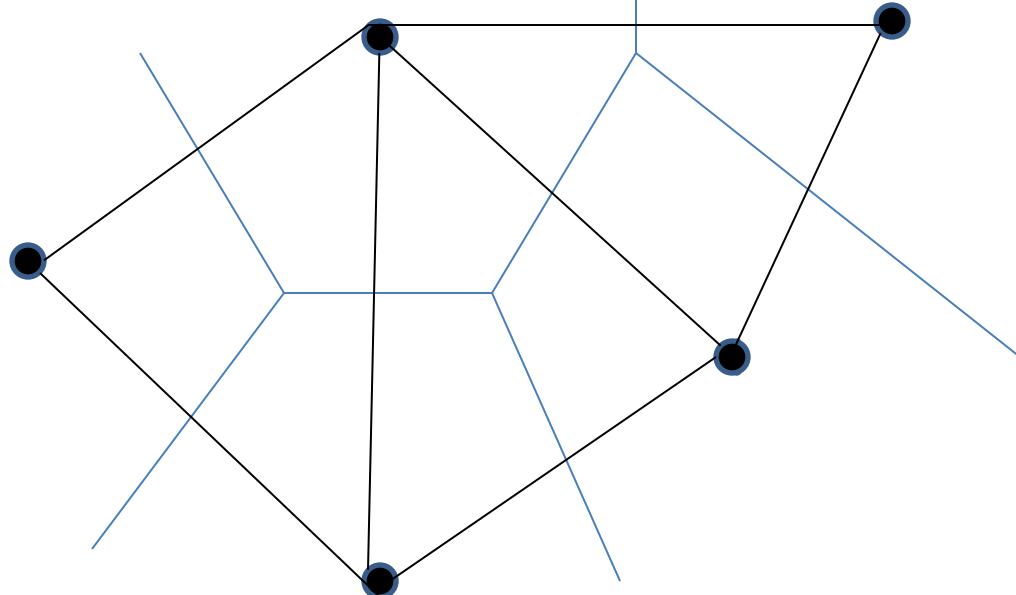
Delaunay Triangulation



Create Voronoi polygons, i.e.

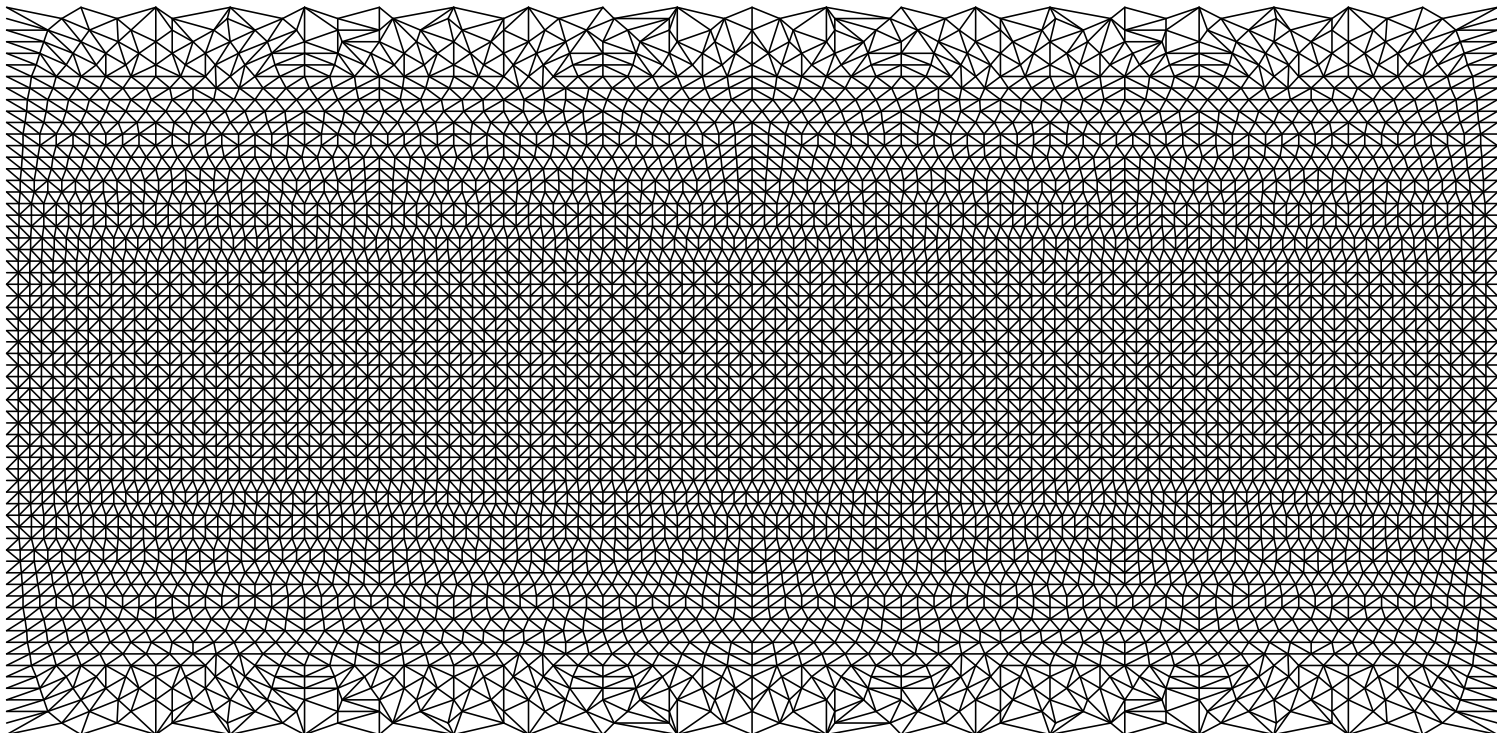
*The construct that assigns to each point the area
of the plane closer to that point than to any other point
in the set. A side of a Voronoi polygon must be midway between the two points
which it separates*

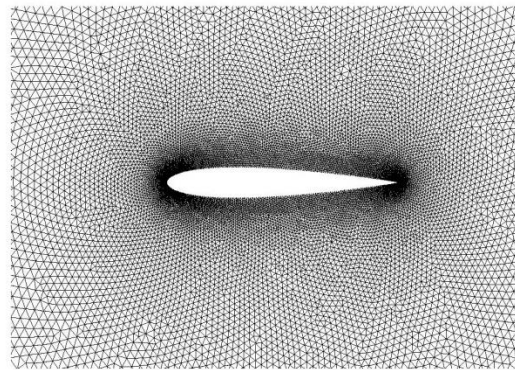
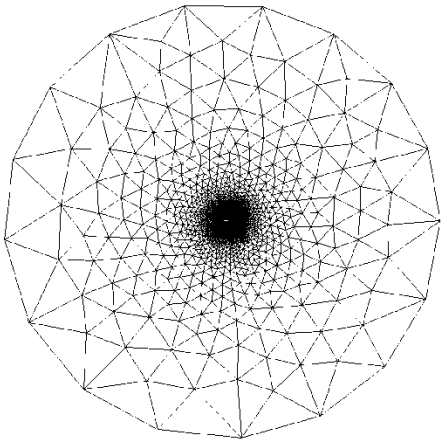
Delaunay Triangulation



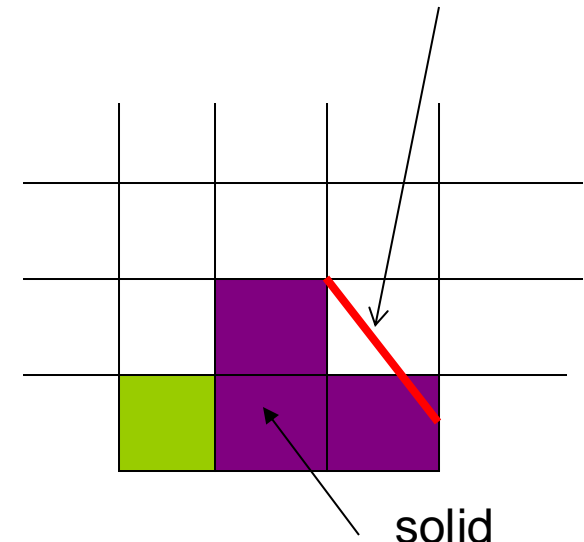
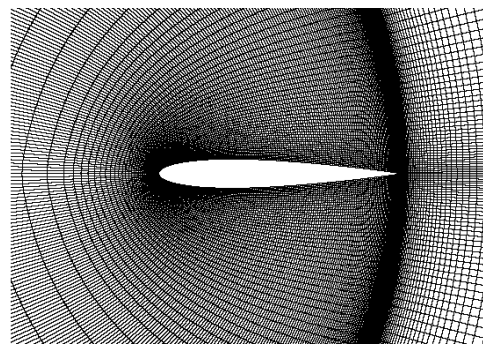
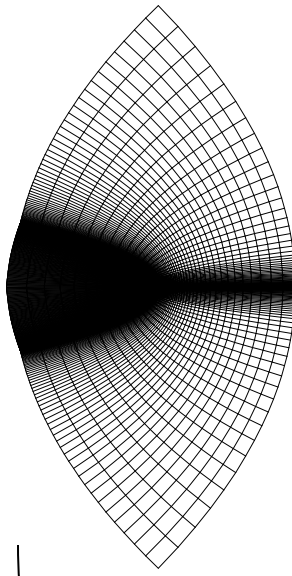
If all point pairs of which have some boundary in common are joint by straight lines, the result is a triangulation of the convex hull of the points.

Delaunay Triangulation mesh constructed from the reduced Gaussian grid points





Fluxes can be
constructed
for the surfaces
which cut cells



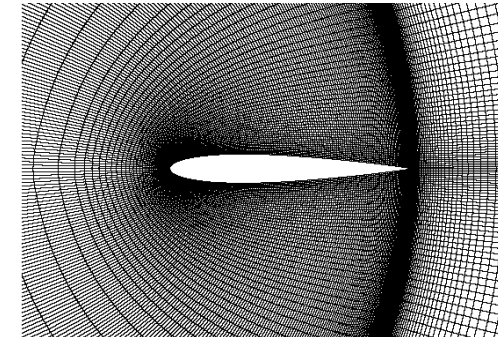
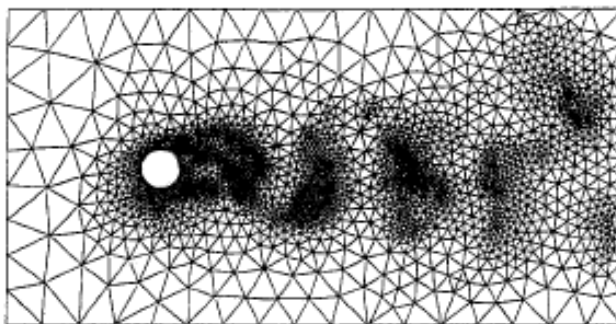
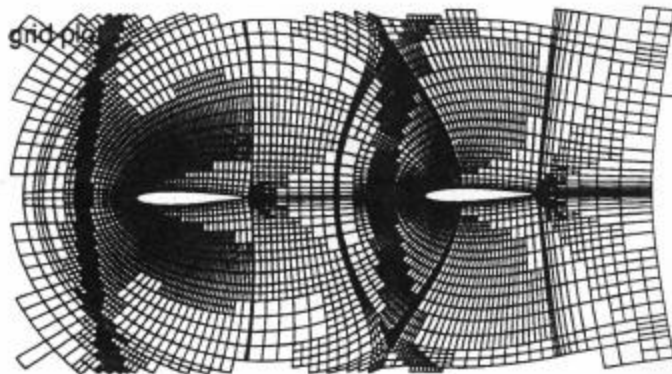
Geometry conforming meshes

Meshing techniques for mesh adaptivity

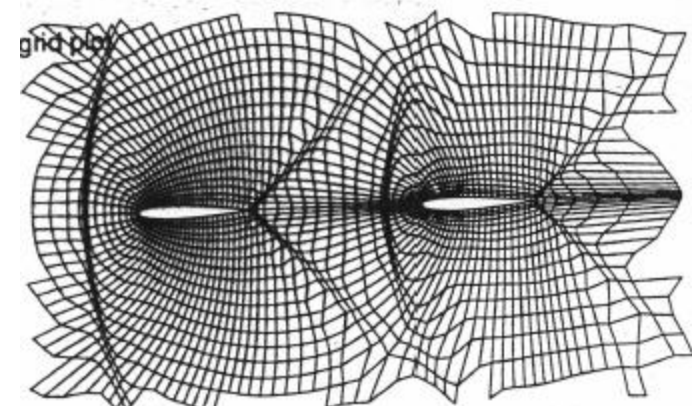
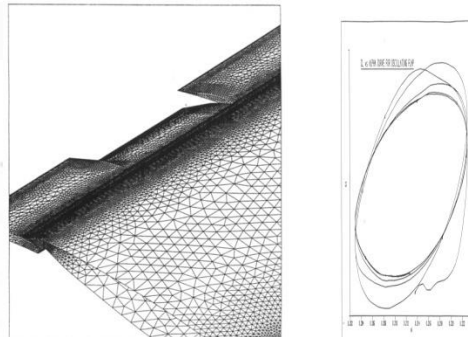
-for lower order elements are:

point enrichment (h-refinement),

and automatic regeneration



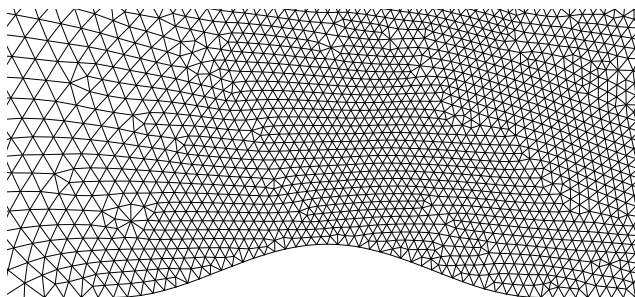
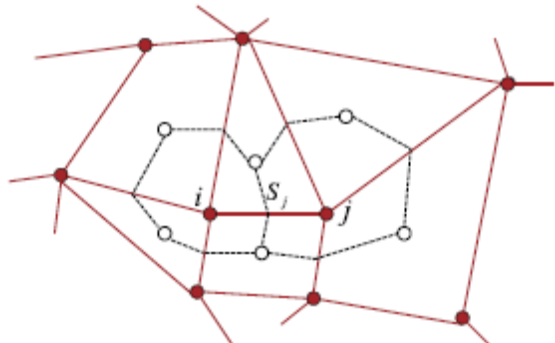
mesh movement



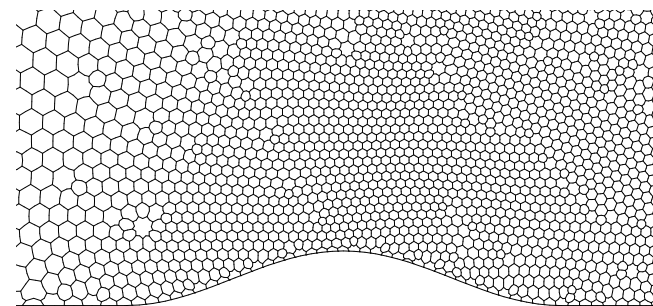
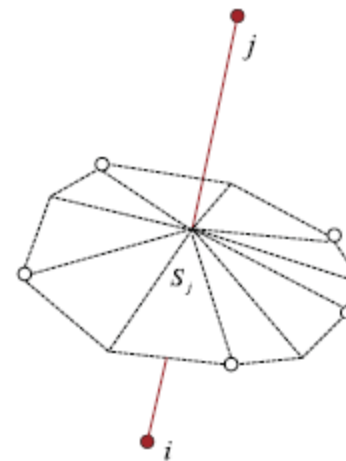
Dynamic regenerations for
Meshes utilising a mapping
are particularly efficient

-for higher order elements
(p-refinement) increases order of shape
function that is the order of polynomial
used for elemental interpolation

The Edge Based Finite Volume Discretisation



Edges

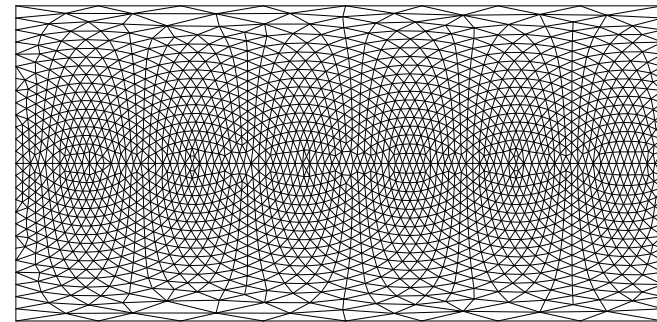
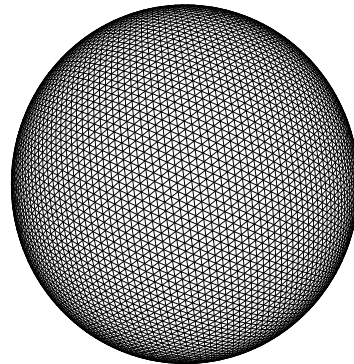


*Median dual computational mesh
Finite volumes*

Geospherical framework

$$\frac{\partial G\Phi}{\partial t} + \nabla \cdot (\mathbf{V}\Phi) = GR$$

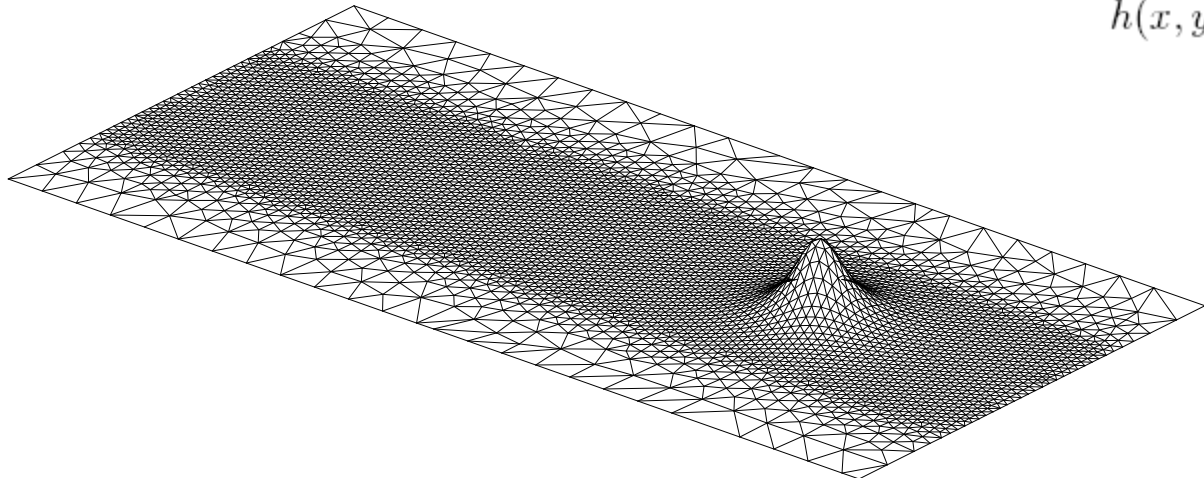
$$\Phi_i^{n+1} = \mathcal{A}_i(\Phi^n + 0.5\delta t R^n, \mathbf{V}^{n+1/2}, G) + 0.5\delta t R_i^{n+1}$$



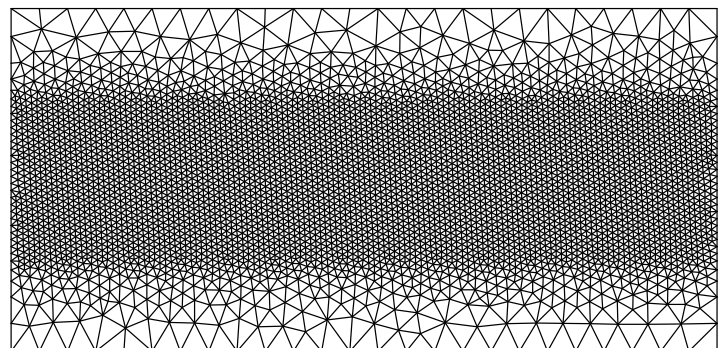
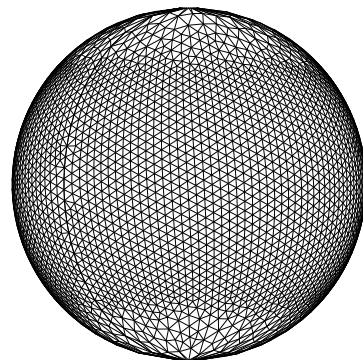
(Szmelter & Smolarkiewicz, J. Comput. Phys. 2010)

A stratified 3D mesoscale flow past an isolated hill

$$h(x, \tilde{y}) = h_0[1. + (l/\mathcal{L})^2]^{-3/2},$$

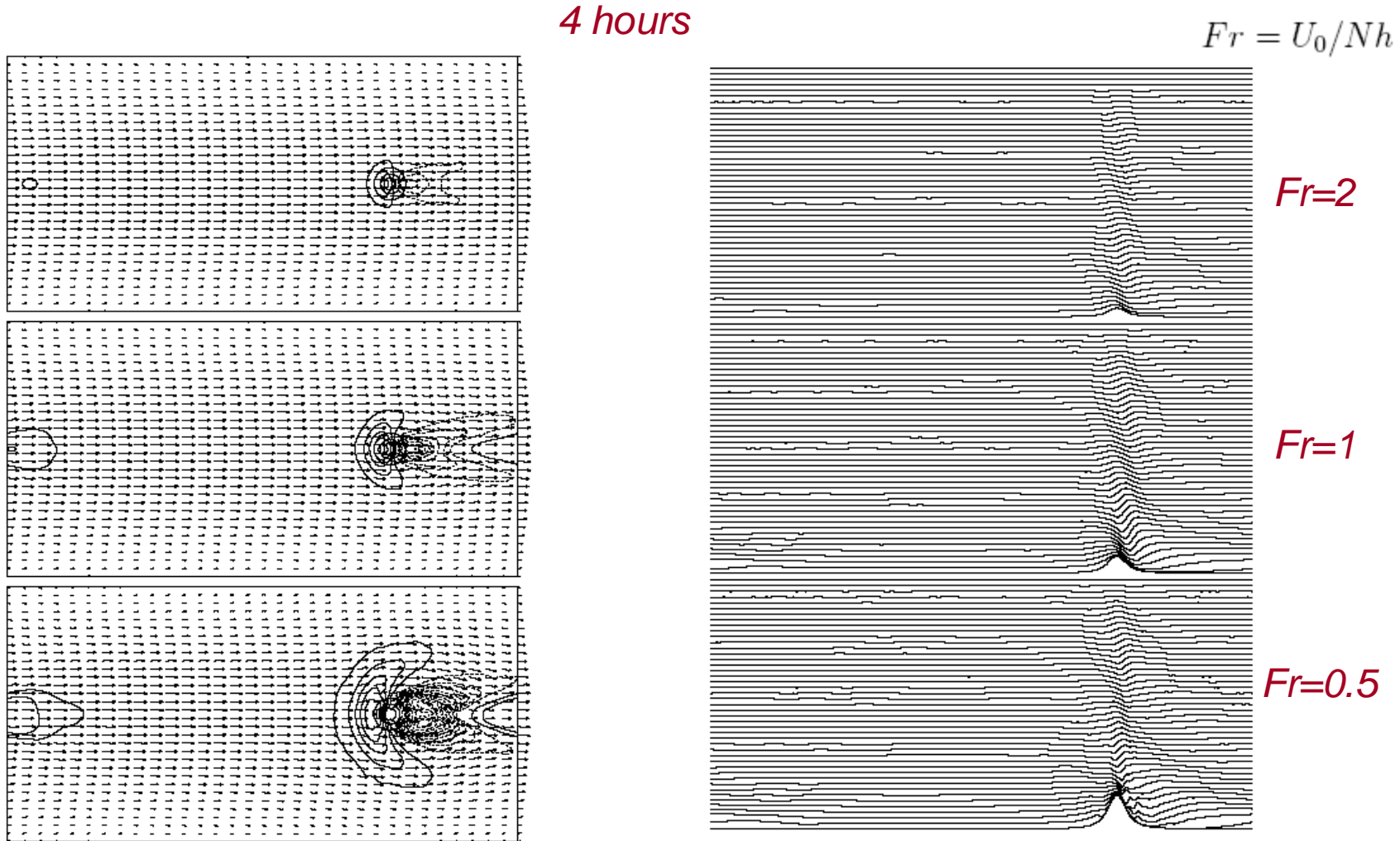


(4532 points)



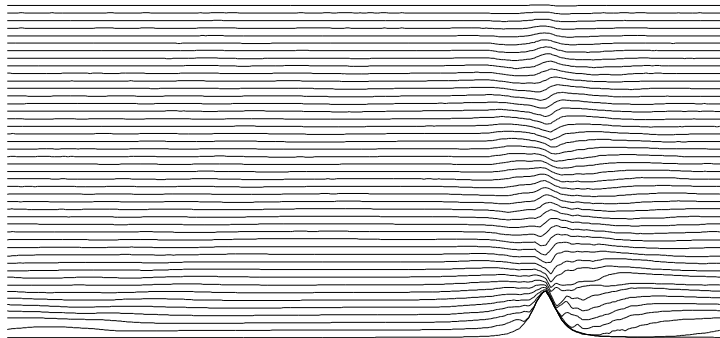
Reduced planets (Wedi & Smolarkiewicz, QJR 2009)

Stratified (mesoscale) flow past an isolated hill on a reduced planet

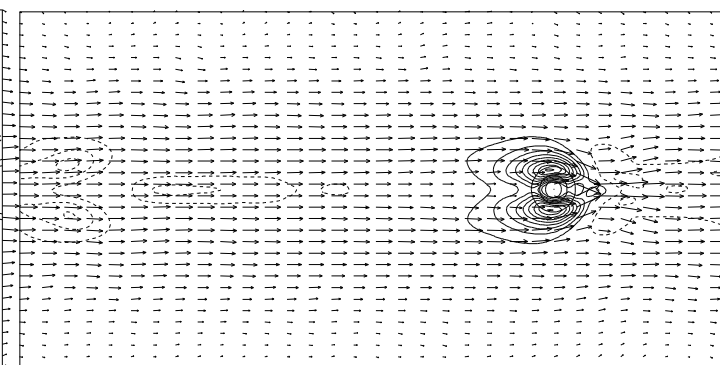
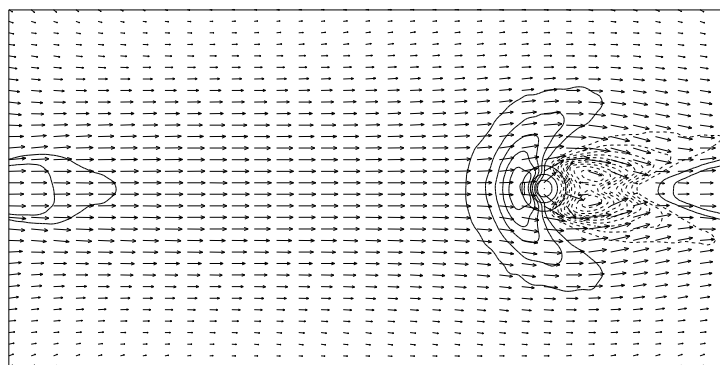
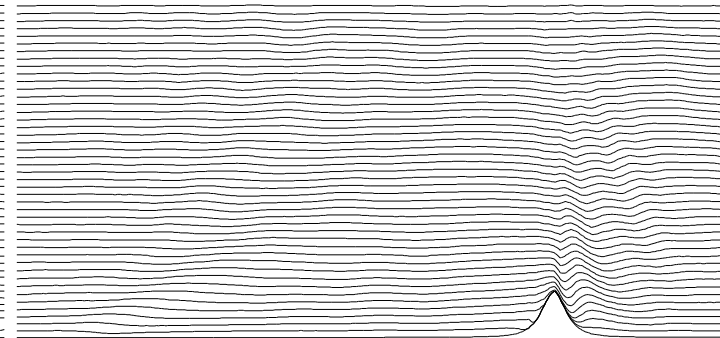


$Fr=0.5$

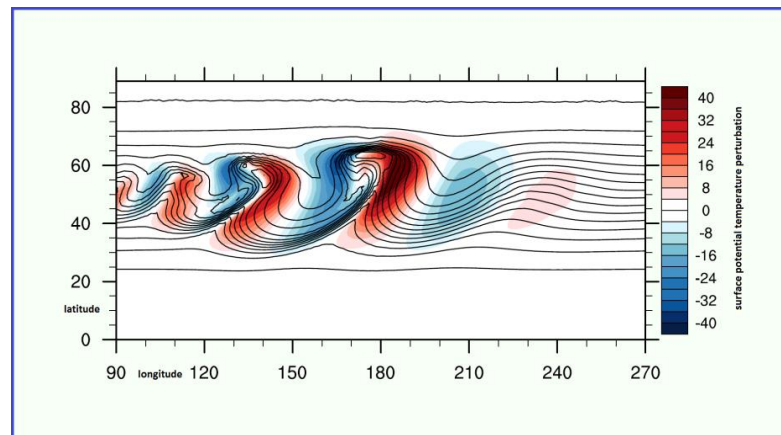
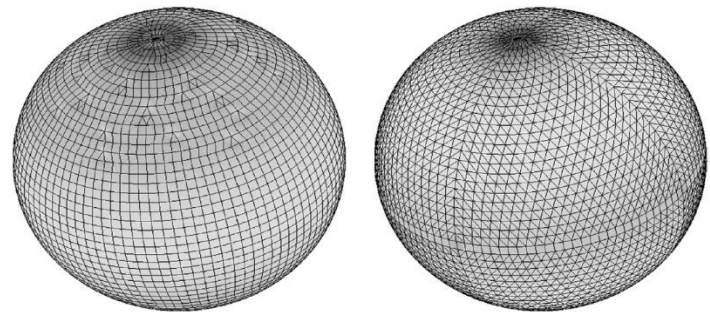
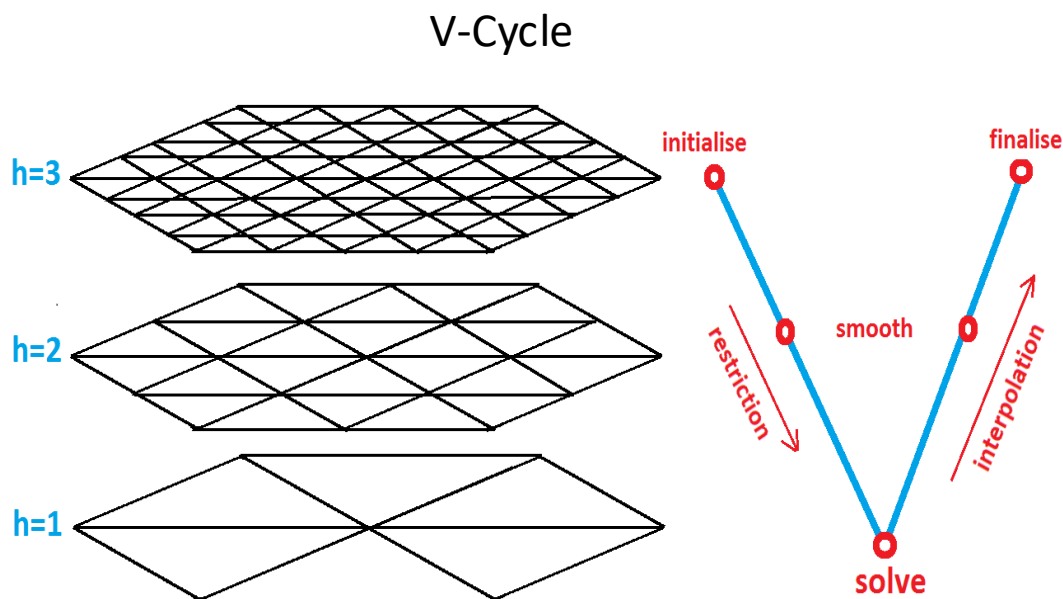
$Ro \gg 1$



$Ro \gtrsim 1$



Multigrid techniques



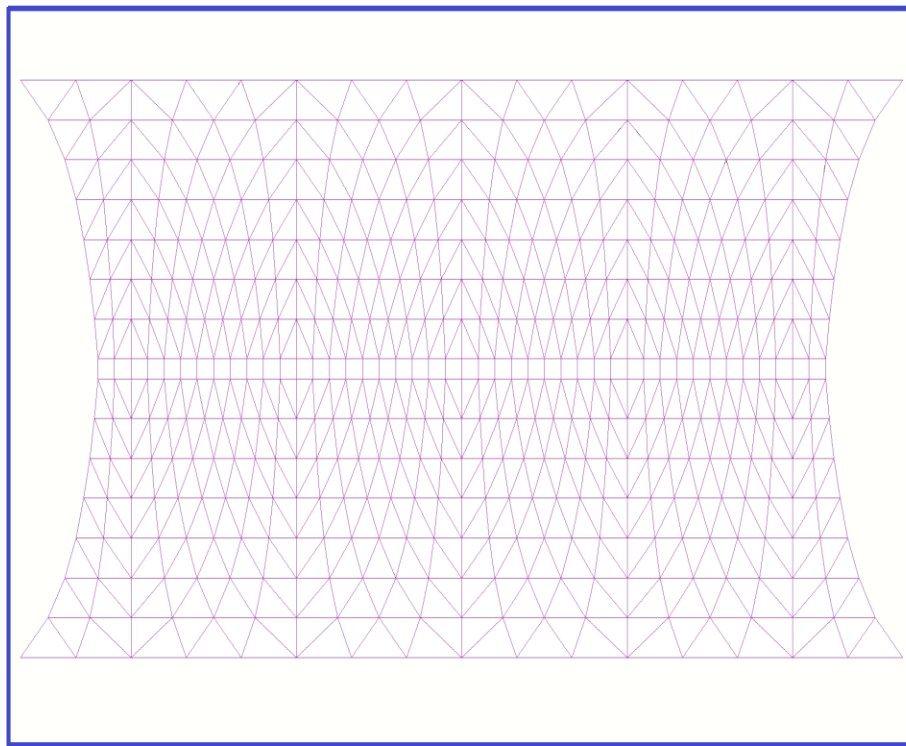
Multigrid using Atlas

Octahedral 16 mesh:

computational domain

Remove odd latitudes

Single level of mesh coarsening



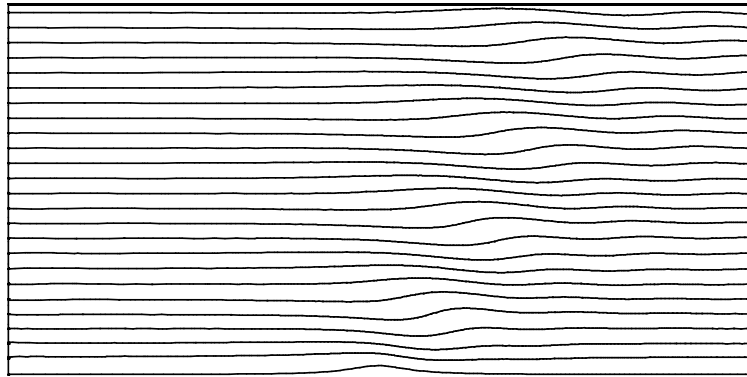
Nonhydrostatic Boussinesq mountain wave

Szmelter & Smolarkiewicz, *Comp. Fluids*, 2011

$$\nabla \bullet (\mathbf{V} \rho_o) = 0 ,$$

$$\frac{\partial \rho_o V^I}{\partial t} + \nabla \bullet (\mathbf{V} \rho_o V^I) = -\rho_o \frac{\partial \tilde{p}}{\partial x^I} + g \rho_o \frac{\theta'}{\theta_o} \delta_{I2}$$

$$\frac{\partial \rho_o \theta}{\partial t} + \nabla \bullet (\mathbf{V} \rho_o \theta) = 0 .$$



$$NL/U_o = 2.4$$

Comparison with the EULAG's (structured mesh) results --- very close

with the linear theories (Smith 1979, Durran 2003):

over 7 wavelengths : 3% in wavelength; 8% in propagation angle; wave amplitude loss 7%

$$\frac{\partial \Phi}{\partial t} + \nabla \bullet (\nabla \Phi) = R$$

Gravity wave breaking in an isothermal stratosphere

$$\nabla \cdot (\bar{\rho} \mathbf{v}) = 0, \quad \frac{D\theta}{Dt} = 0, \quad \frac{D\mathbf{v}}{Dt} = -\nabla \Phi' - g \frac{\theta'}{\bar{\theta}}, \quad \text{Lipps \& Hemler}$$

$$\nabla \cdot (\bar{\rho} \bar{\theta} \mathbf{v}) = 0, \quad \frac{D\theta}{Dt} = 0, \quad \frac{D\mathbf{v}}{Dt} = -c_p \theta \nabla \pi' - g \frac{\theta'}{\bar{\theta}} \quad \text{Durran}$$

$$D\psi/Dt = R$$

by combining $\rho^* \cdot (D\psi/Dt = R)$ with $\psi \cdot (\nabla \rho^* \mathbf{v} = 0)$,

$$\frac{\partial \rho^* \psi}{\partial t} + \nabla \cdot (\rho^* \mathbf{v} \psi) = \rho^* R.$$

$$\psi_t^{n+1} = \mathcal{A}_t(\tilde{\psi}, \mathbf{v}^{n+1/2}, \rho^*) + 0.5\delta t R_t^{n+1}$$

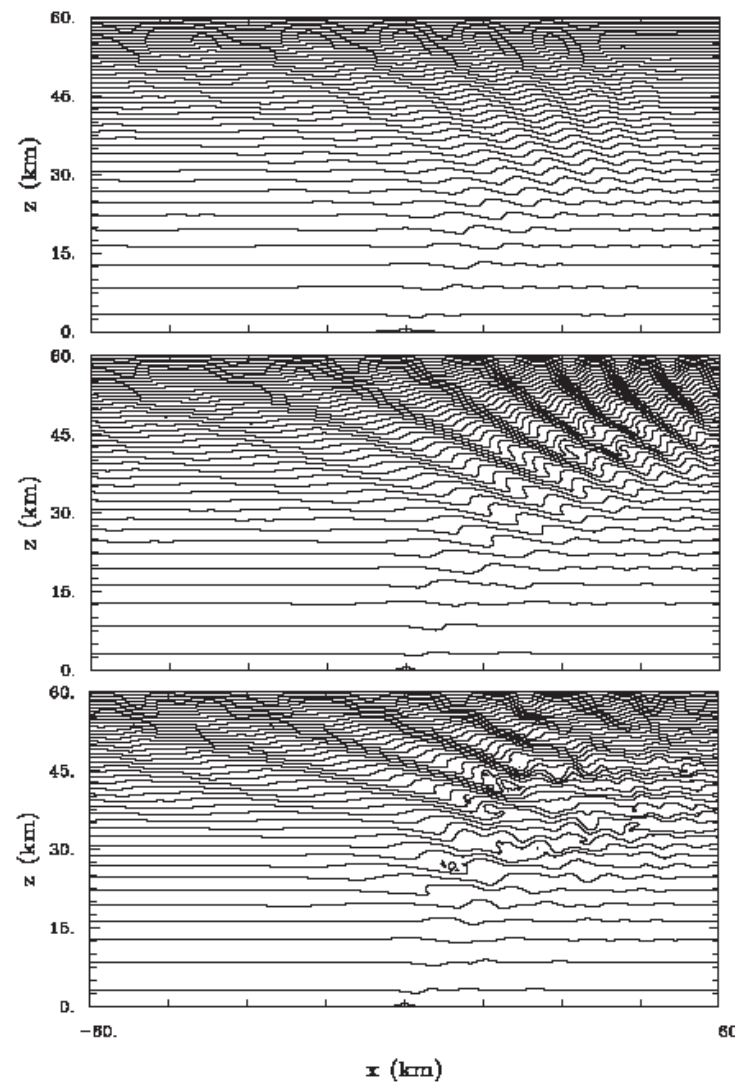
$$S_\theta = d \ln \bar{\theta} / dz = 4.4 \cdot 10^{-5} \text{ m}^{-1}$$

$$\mathbf{v}_e = (u_e, 0) \quad u_e = U = 20 \text{ ms}^{-1}$$

(Prusa et al JAS 1996,
Smolarkiewicz & Margolin, Atmos. Ocean
1997

Klein, Ann. Rev. Fluid Dyn., 2010,
Smolarkiewicz et al Acta Geoph 2011)

Isentropes at $t = 60, 90, \text{ and } 120 \text{ min.}$

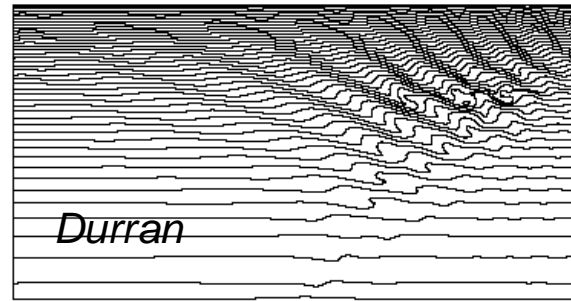
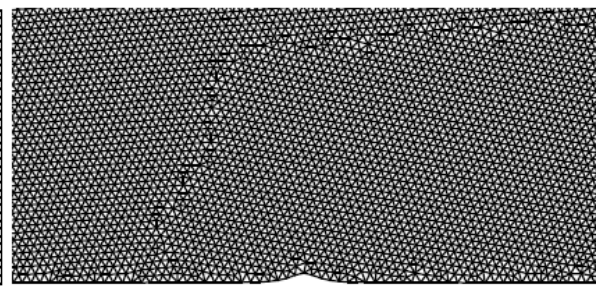
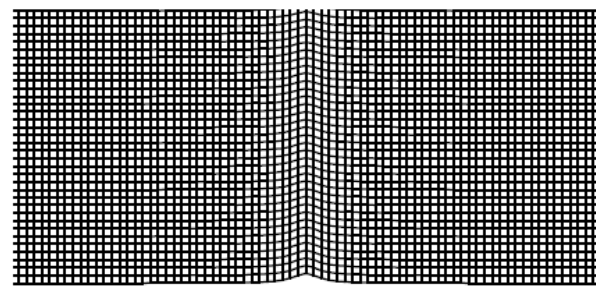
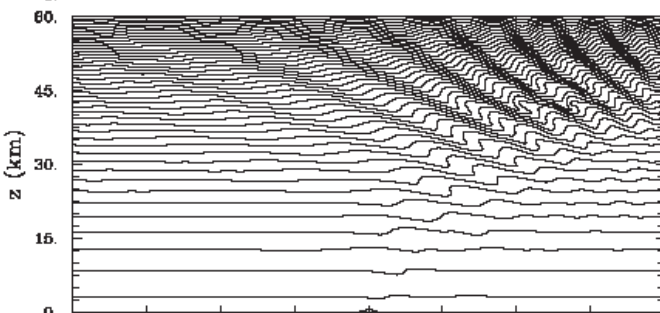


Gravity wave breaking in an isothermal stratosphere

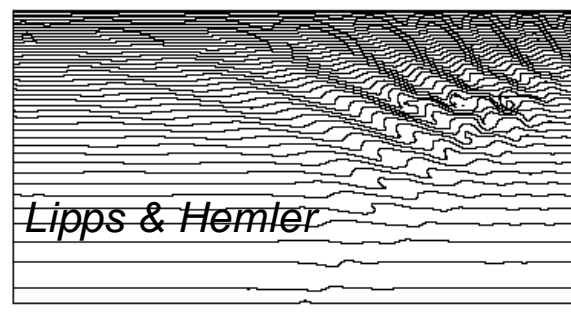
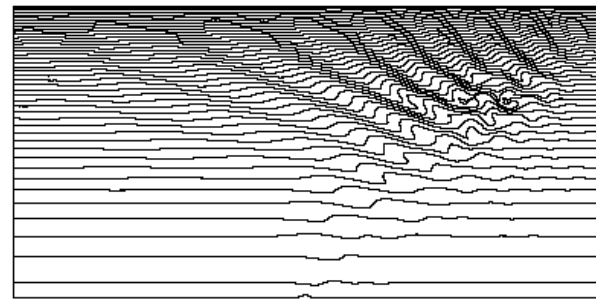
Nonhydrostatic Edge-Based NFT

Isentropes at $t = 90$ min

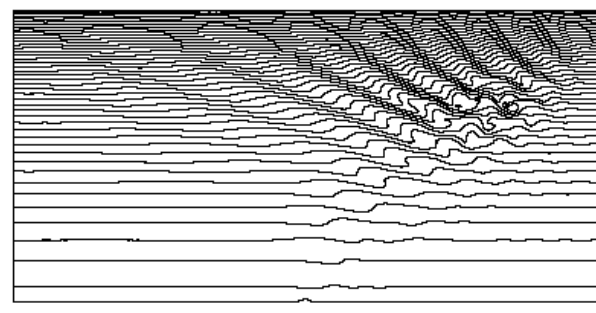
EULAG *CV/GRID*



Durran



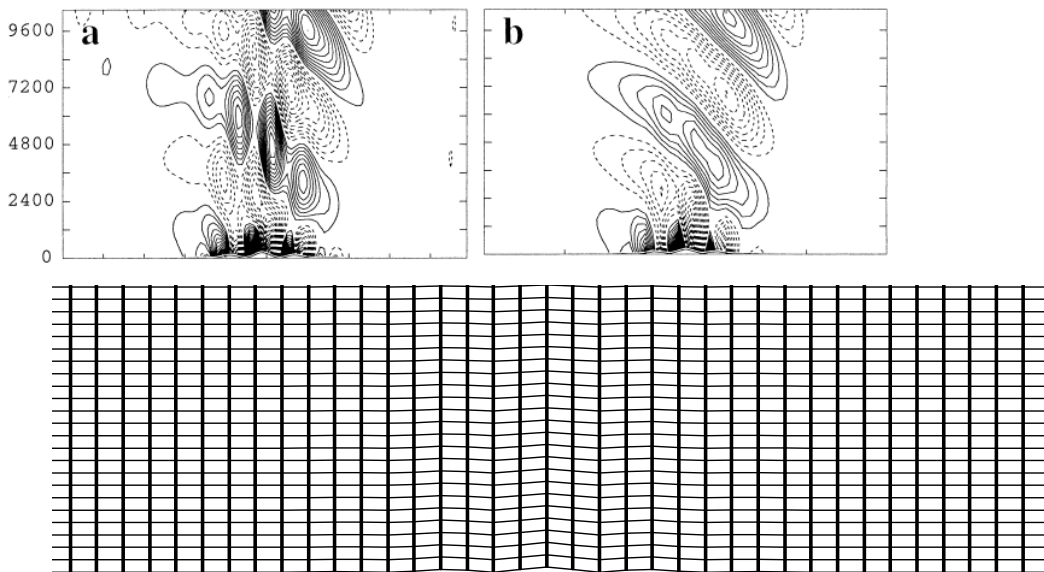
Lipps & Hemler



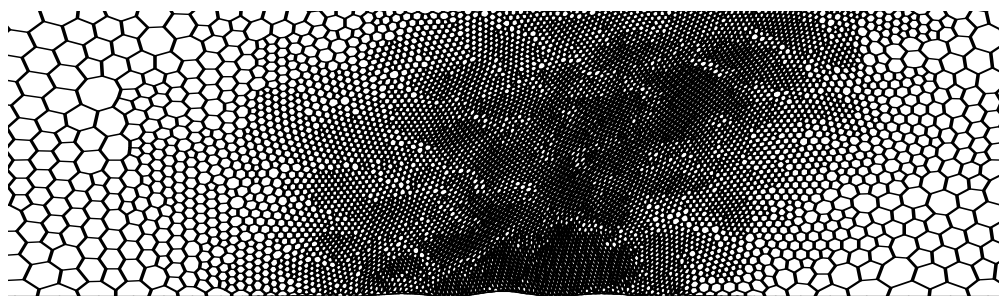
Static mesh adaptivity with MPDATA based error indicator

Schär Mon. Wea. Rev. 2002

(Recommended mesh ca10000 points)



Coarse initial mesh $80 \times 45 = 3600$ points and solution



Adapted mesh 8662 points and solution

Szmelter et al JCP 2015

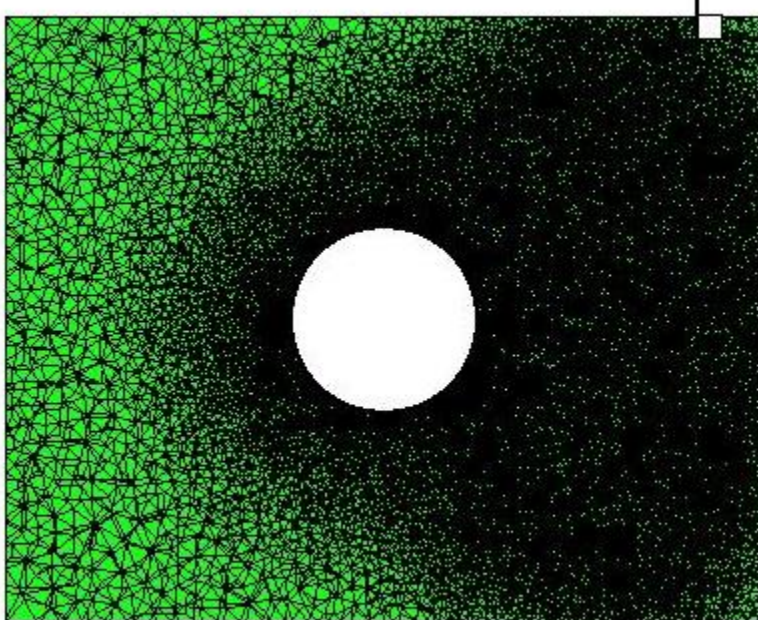
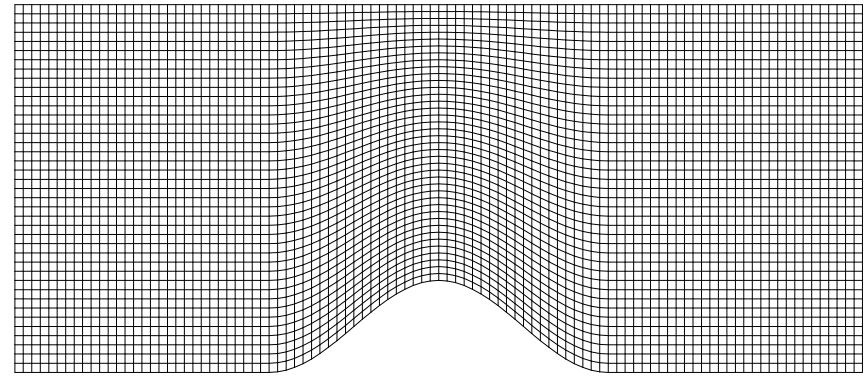
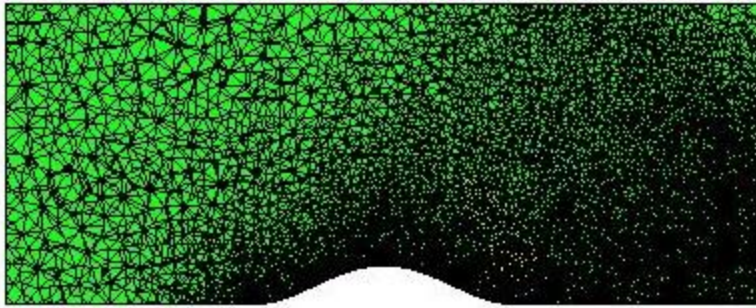
1121192 Cartesian

$dx=100$

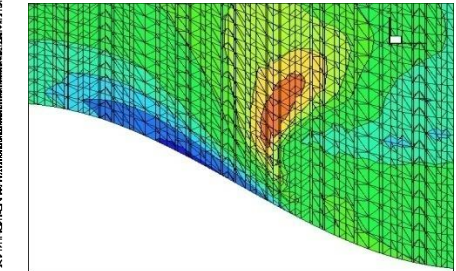
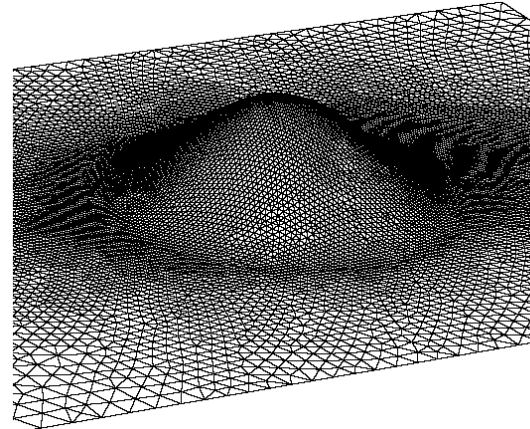
692533 Distorted prisms $dx=100-400$

441645 tetra $dx=50 -450$

Stratified flow past a steep isolated hill

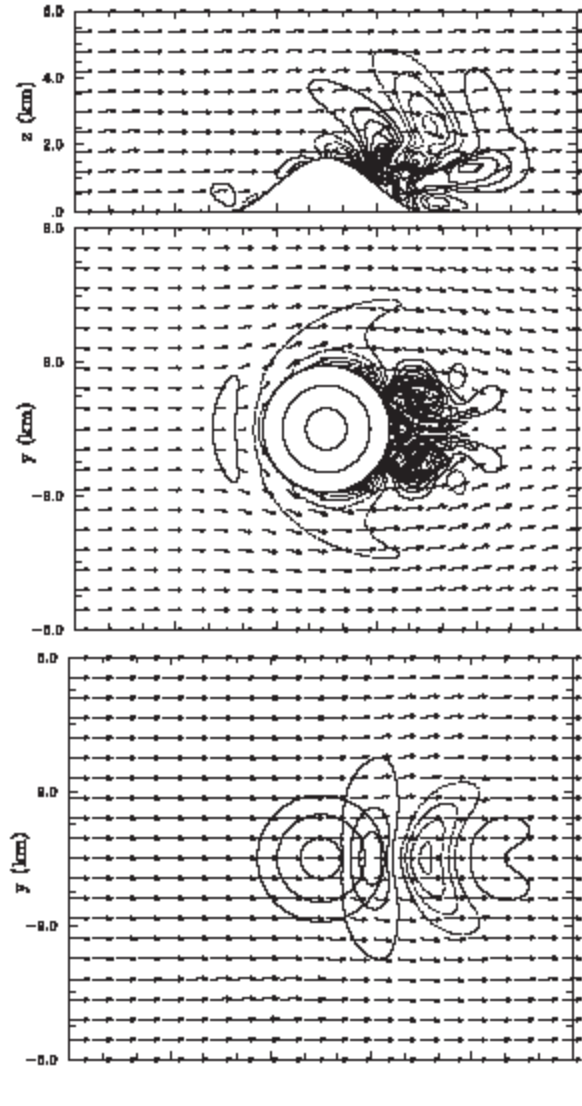


$$z_{i,k} = (k - 1)\delta z \left(1 - \frac{h_i}{H}\right) + h_i ,$$

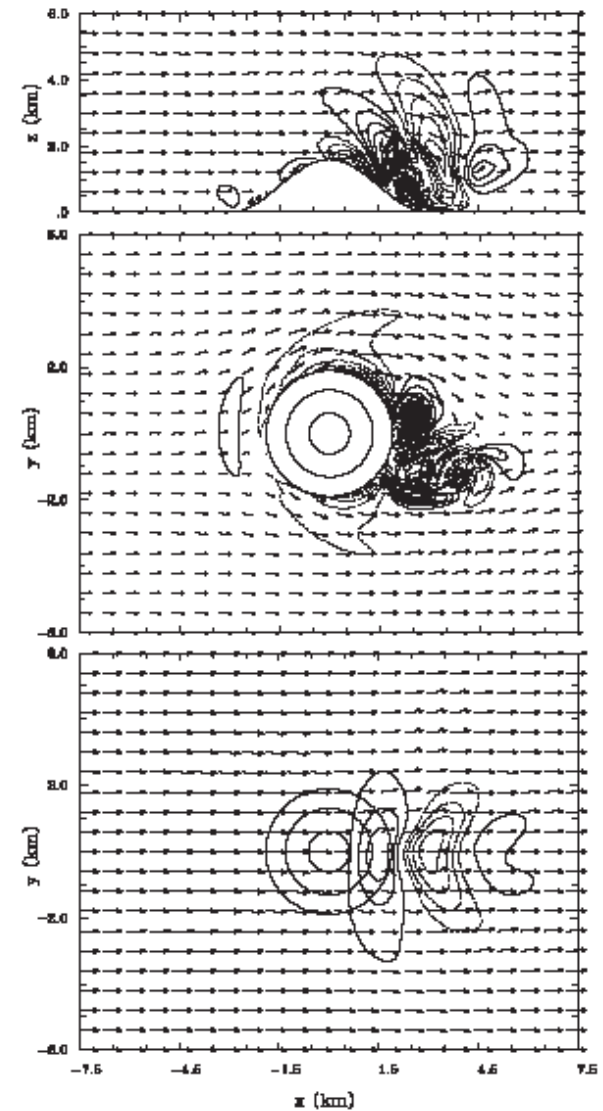


Stratified flow past a steep isolated hill

Hunt & Snyder JFM 1980
Smolarkiewicz & Rotuno
JAS 1989



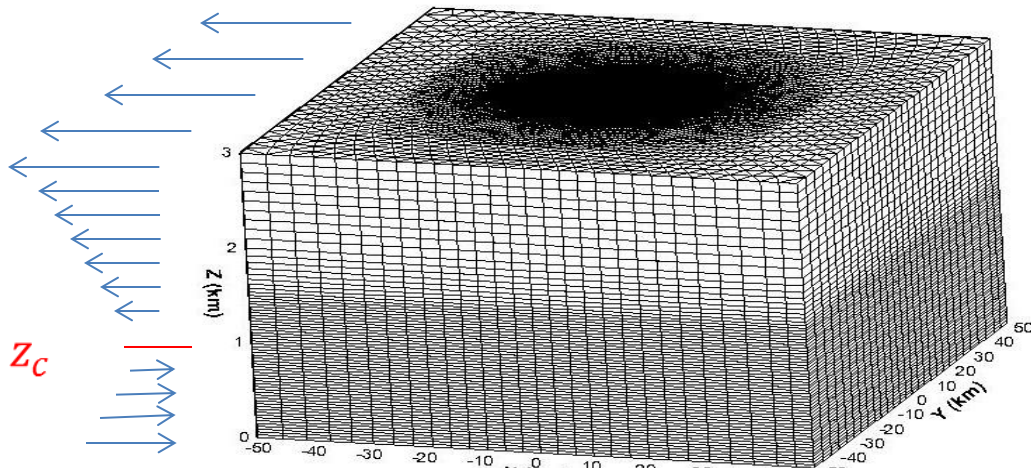
$$Fr = 1/3, \quad Ro \nearrow \infty$$



$$Fr = 1/3, \quad Ro \approx 3$$

The effect of critical levels on stratified flows past an axisymmetric mountain

Szmelter et. al. JCP 2015



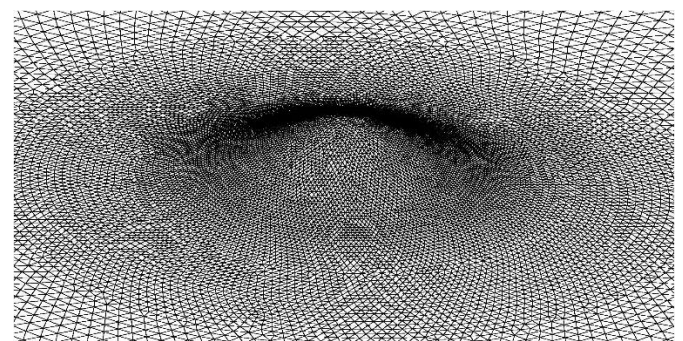
$$U_0 = 10 \text{ ms}^{-1}, \quad U(z) = U_0 \left(1 - \frac{z}{z_c}\right)$$

$$\frac{U_0}{N_a} = 0.2, \quad R_i = \left(\frac{N z_c}{U_0}\right)^2 = 1, \quad N = 0.01 \text{ s}^{-1}$$

$$a = 5000 \text{ m}, \quad h(r) = h_0 \left(1 + \frac{r^2}{a^2}\right)^{-\frac{3}{2}}, \quad r \equiv \sqrt{x^2 + y^2}$$

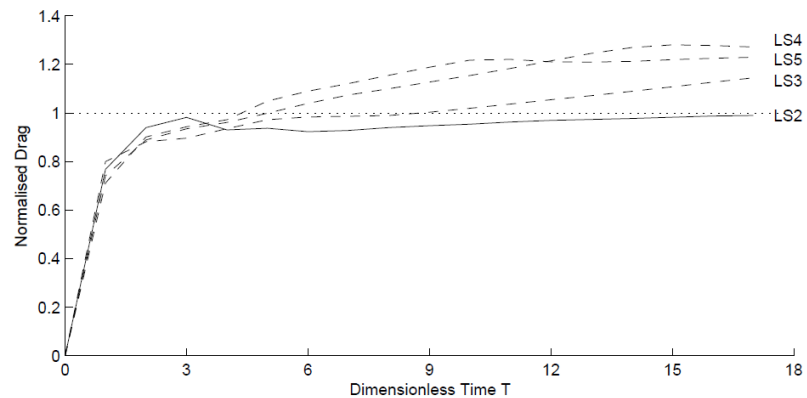
Prismatic mesh

$$\begin{aligned} \tilde{z}_{i,k} &= \tilde{z}_{i,k-1} + \delta \tilde{z}_k \\ \tilde{z}_{i,k} &= \tilde{z}_{i,k} \left(1 - \frac{h_i}{H}\right) + h_i \end{aligned}$$



Triangular surface mesh

The effect of critical levels on stratified flows past an axisymmetric mountain



$$\hat{h} = \frac{h_0 N}{U_0} \quad T = \frac{t U_0}{a}$$

Experiment	Ri	\hat{h}	$D/D_0(6)$	$D/D_0(10)$	$D/D_0(18)$
LS2 (linear)	1	0.05	0.923	0.954	0.997
LS3 (nonlinear)	1	0.1	0.983	1.02	1.160
LS4 (nonlinear)	1	0.2	1.04	1.15	1.26
LS5 (nonlinear)	1	0.3	1.09	1.22	1.23

The effect of critical levels on stratified flows past an axisymmetric mountain

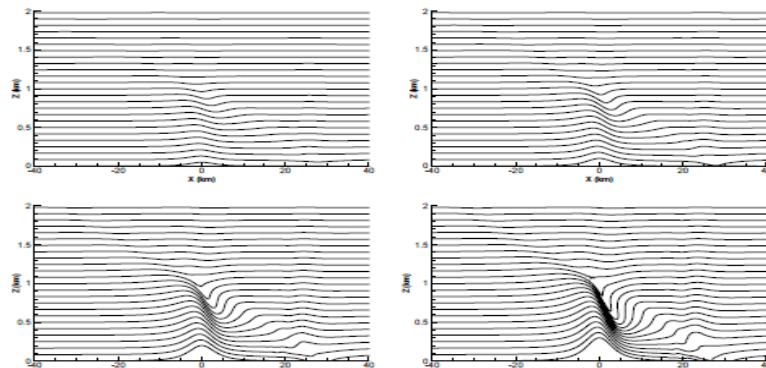


Fig. 12. Isentropes at $T=6$ in $y = 0$ vertical plane for experiments LS2 (left, top), LS3 (right, top), LS4 (left, bottom) and LS5 (right, bottom).

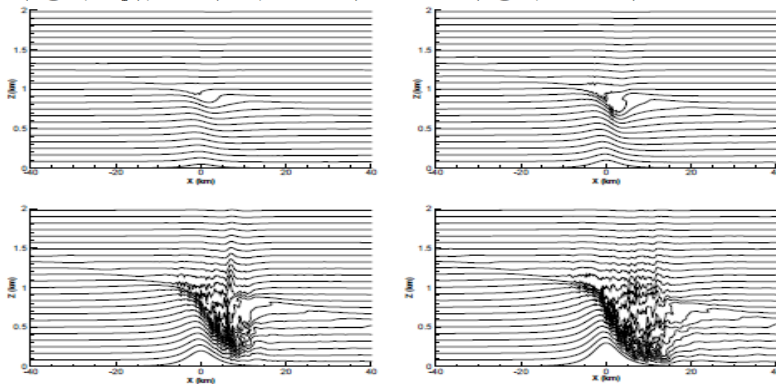
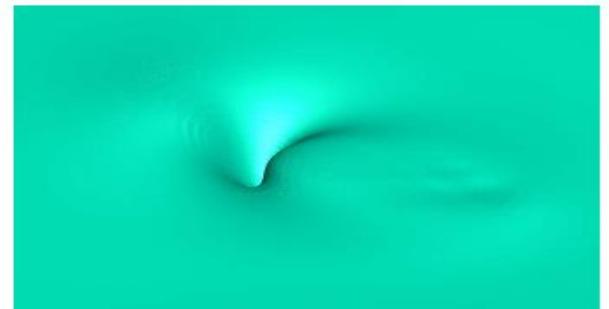
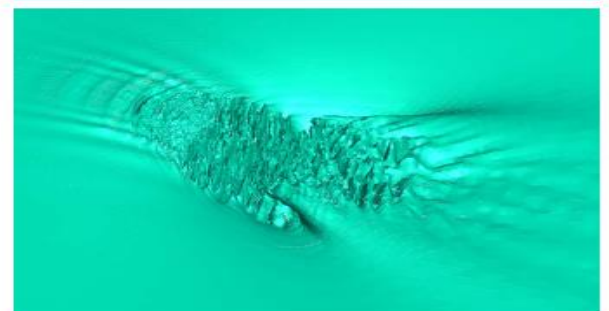


Fig. 13. As in Fig. 12 but at $T=18$.

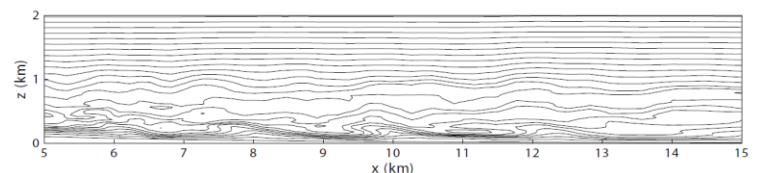


$T = 6$

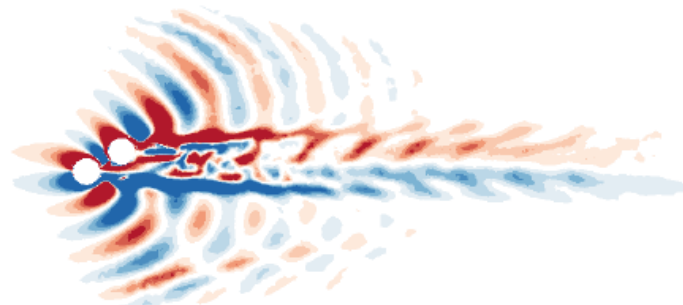
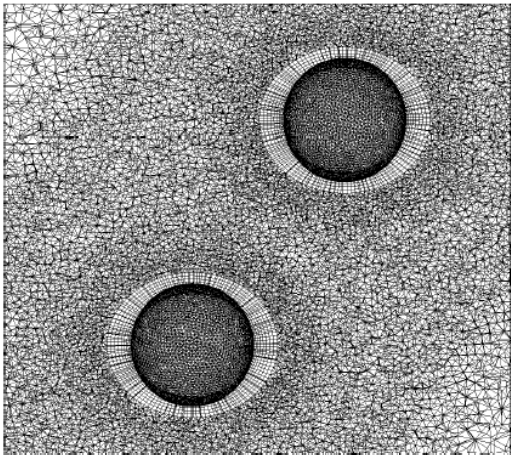


$T = 18$

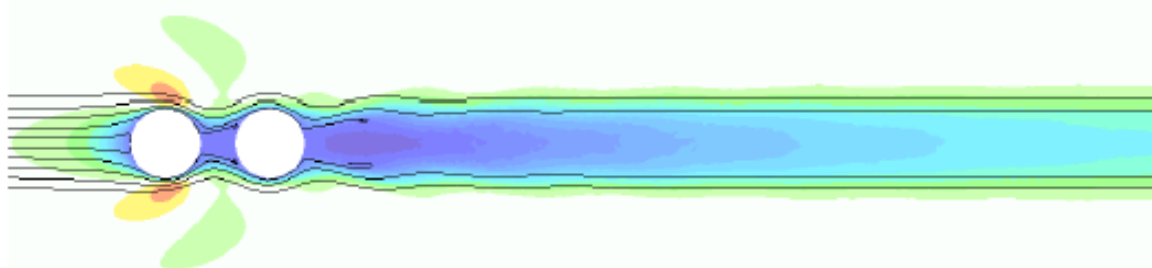
the isentrope with undisturbed height $z = 0.94z_c$ LS5.



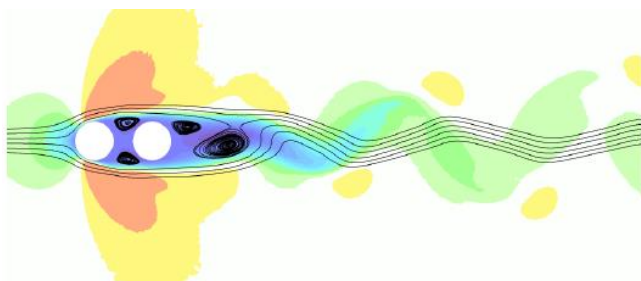
*Stratified flow past two spheres,
 $Fr=0.625$, $Re=300$*



$Fr=0.625$
Tilted
configuration



$Fr=0.625$

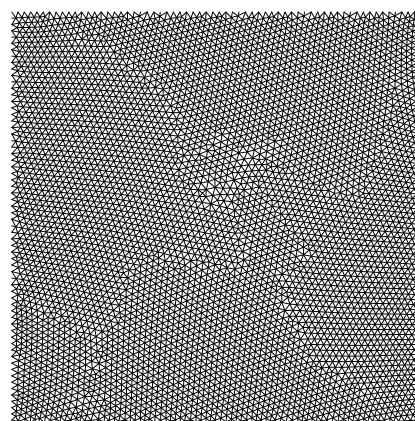
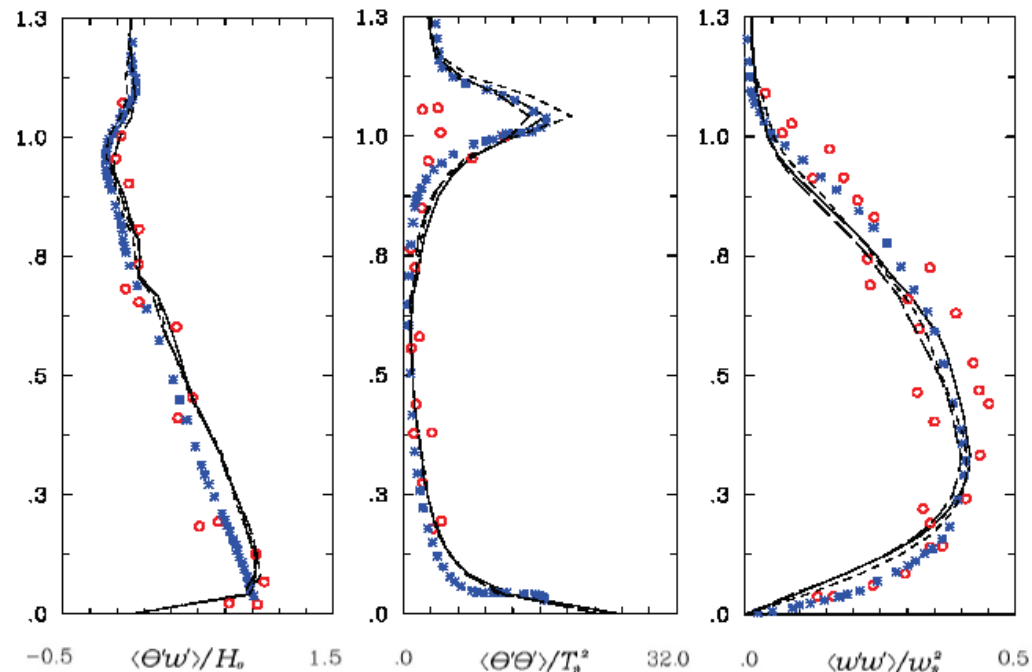
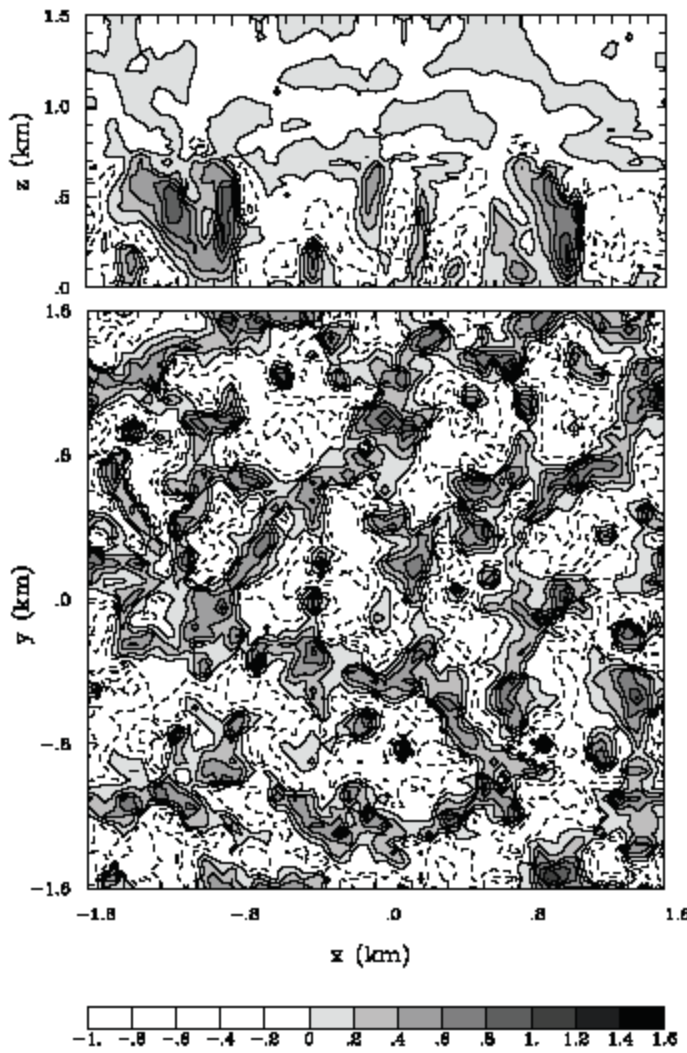


$Fr=0.25$

Convective Planetary Boundary Layer

Schmidt & Schumann JFM 1989

Smolarkiewicz et al JCP 2013



<i>Edge-based T</i>	—
<i>Edge-based C</i>	- - -
<i>EULAG</i>	- · -
<i>SS LES</i>	* *
<i>Observation</i>	○ ○
<i>64x64x51</i>	

Selected references for further details

- Cocetta F, Szmelter J, Gillard M (2021) Simulations of stably stratified flow past two spheres at Re=300, *Physics of Fluids*, 334, 046602.
- Smolarkiewicz, PK, Szmelter, J, Xiao, F (2016) Simulation of all-scale atmospheric dynamics on unstructured meshes, *Journal of Computational Physics*, 322, pp.267-287
- Szmelter, J, Zhang, Z, Smolarkiewicz, PK, (2015) An unstructured-mesh atmospheric model for nonhydrostatic dynamics: Towards optimal mesh resolution, *Journal of Computational Physics*, 249, pp.363-381
- Smolarkiewicz, PK, Szmelter, J, Wyszogrodzki, AA (2013) An unstructured-mesh atmospheric model for nonhydrostatic dynamics, *Journal of Computational Physics*, 254, pp.184-199
- Smolarkiewicz, PK and Szmelter, J (2011) A Nonhydrostatic Unstructured-Mesh Soundproof Model for Simulation of Internal Gravity Waves, *Acta Geophysica*, 59(6), pp.1109-1134
- Szmelter, J and Smolarkiewicz, PK (2011) An edge-based unstructured mesh framework for atmospheric flows, *Computers and Fluids*, 46(1), pp.455-460.
- Szmelter, J and Smolarkiewicz, PK (2010) An edge-based unstructured mesh discretisation in geospherical framework, *Journal of Computational Physics*, 229, pp.4980-4995.
- Smolarkiewicz, PK and Szmelter, J (2009) Iterated upwind schemes for gas dynamics, *Journal of Computational Physics*, 228(1), pp.33-54
- Smolarkiewicz, PK and Szmelter, J (2008) An MPDATA-based solver for compressible flows, *International Journal for Numerical Methods in Fluids*, 56(8), pp.1529-1534
- Szmelter, J and Smolarkiewicz, PK (2006) MPDATA error estimator for mesh adaptivity, *International Journal for Numerical Methods in Fluids*, 50(10), pp.1269-1293
- Smolarkiewicz, PK and Szmelter, J (2005) MPDATA: An Edge-Based Unstructured-Grid Formulation, *Journal of Computational Physics*, 206(2), pp.624-649
- Zienkiewicz OC, Taylor RL, The Finite Element Method, 5th Ed, Butterworth-Heinemann, (2000)
- Szmelter, J, Marchant, MJ, Evans, A, Weatherill, NP (1992) Two-dimensional Navier-Stokes Equations - Adaptivity on Structured Meshes, *Comp. Meth. Appl. Mech. Eng*, 101, pp.355-368.
- Evans, A, Marchant, MJ, Szmelter, J, Weatherill, NP (1991) Adaptivity for Compressible Flow Computations Using Point Embedding on 2-D Structured Multiblock Meshes, *International Journal for Numerical Methods in Engineering*, 32, pp.896-919
- Wu, J, Zhu, JZ, Szmelter, J, Zienkiewicz, OC (1990) Error Estimation and Adaptivity in Navier-Stokes Incompressible Flows, *Computational Mechanics*, 6, pp.259-270.